CHAPTER

6 Crack Tip Plasticity

We have so far introduced fracture in solids undergoing linearly elastic deformations. Most engineering materials, however, exhibit various degrees of nonlinear constitutive behavior when stresses exceed a critical level. Figure 6.1 shows the typical uniaxial stress–strain curve for metals. Under loading conditions, the stress–strain relationship deviates from Hooke's law once the uniaxial stress exceeds σ_Y, which is called the yield stress. When unloading occurs at point B, the stress–strain curve follows a linear path (BB') with the slope approximately equal to the Young's modulus.

It is known from Chapter 3 that linear elastic fracture mechanics (LEFM) predicts an inverse square-root singularity at a crack tip. The stress singularity implies that the elastic stress will exceed the yield stress when approaching the crack tip, and consequently, a plastic zone develops in the crack tip region. This chapter discusses the plasticity effects around a crack tip, for example, the stress and deformation fields,

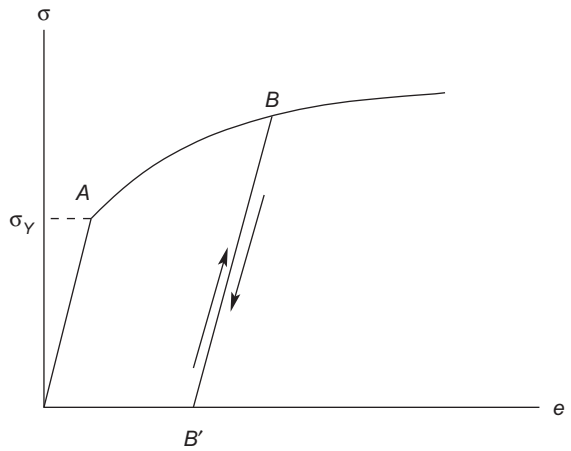

FIGURE 6.1

Uniaxial stress–strain curve for typical metals.

Fracture Mechanics. DOI: 10.1016/B978-0-12-385001-0.00006-7

plastic zone size and shape, and crack tip opening displacement (CTOD). Crack initiation and growth based on these results will be discussed in Chapter 7.

6.1 YIELD CRITERIA

A yield criterion describes a condition on stresses that separates the elastic and plastic states. For the uniaxial stress state, the yield ciriterion is simply expressed as

$$\sigma = \sigma_Y$$

where σ_Y is the uniaxial yield stress; see Figure 6.1. The elastic state corresponds to $\sigma < \sigma_Y$, while the plastic deformation state prevails if $\sigma \geq \sigma_Y$. For a general three-dimensional stress state, a yield criterion is often expressed as

$$Y(\sigma_{ij}) = k$$

where Y represents a function of stresses and k is a constant. Yielding occurs if the yield criterion is satisfied. Among various yield criteria proposed, the Tresca and the von Mises criteria are most commonly used.

6.1.1 Tresca Yield Criterion

The Tresca yield criterion is based on the assumption that material yielding results from pure shear. In terms of principal stresses σ_1, σ_2, and σ_3, the maximum shear stress is among the following three quantities:

$$\tau_1 = \frac{1}{2}|\sigma_2 - \sigma_3|, \quad \tau_2 = \frac{1}{2}|\sigma_1 - \sigma_3|, \quad \tau_3 = \frac{1}{2}|\sigma_1 - \sigma_2|$$

which occur in three orthogonal planes. The Tresca criterion states that yielding occurs if the maximum shear stress reaches a critical value and can be expressed as

$$\begin{aligned} |\sigma_2 - \sigma_3| &= 2\tau_{cr}, \quad \text{or} \\ |\sigma_1 - \sigma_3| &= 2\tau_{cr}, \quad \text{or} \\ |\sigma_1 - \sigma_2| &= 2\tau_{cr} \end{aligned} \tag{6.1}$$

where τ_{cr} is the critical shear stress. The critical value τ_{cr} can be determined using a simple tension test in which yielding is known to occur at $\sigma_1 = \sigma_Y$ and $\sigma_2 = \sigma_3 = 0$. The last two equations in Eq. (6.1) now become

$$|\sigma_1| = 2\tau_{cr} = \sigma_Y$$

We thus have the critical shear stress

$$\tau_{cr} = \frac{\sigma_Y}{2} \tag{6.2}$$

6.1.2 von Mises Yield Criterion

The von Mises yield criterion assumes that material yielding is a result of distortional deformation and is independent of dilational deformation. The strain energy density W for linear elastic materials is given by

$$W = \frac{1}{2}\sigma_{ij}e_{ij}$$

Using Hooke's law, the strain energy density can be expressed in terms of the principal stresses σ_1, σ_2, and σ_3 as

$$W = \frac{1}{12\mu}\left[(\sigma_1-\sigma_2)^2+(\sigma_2-\sigma_3)^2+(\sigma_1-\sigma_3)^2\right]+\frac{1}{18K}(\sigma_1+\sigma_2+\sigma_3)^2$$

where μ is the shear modulus and K is the bulk modulus. The second term associated with K in the preceding expression represents the strain energy due to volume change (dilatational deformation), and the first term represents the distortional energy W_d. The von Mises yield criterion states that yielding occurs if

$$W_d = \frac{1}{12\mu}\left[(\sigma_1-\sigma_2)^2+(\sigma_2-\sigma_3)^2+(\sigma_1-\sigma_3)^2\right] = W_{cr} \tag{6.3}$$

The critical value W_{cr} can also be obtained from a uniaxial tension test with the result

$$W_{cr} = \frac{1}{6\mu}\sigma_Y^2$$

With this determined W_{cr}, Eq. (6.3) can be rewritten as

$$\frac{1}{2}\left[(\sigma_1-\sigma_2)^2+(\sigma_2-\sigma_3)^2+(\sigma_1-\sigma_3)^2\right] = \sigma_Y^2 \tag{6.4}$$

The von Mises criterion can also be expressed in terms of stress components in an arbitrary Cartesian coordinate system (x,y,z):

$$\frac{1}{2}\left[(\sigma_{xx}-\sigma_{yy})^2+(\sigma_{yy}-\sigma_{zz})^2+(\sigma_{zz}-\sigma_{xx})^2+6({\sigma_{xy}}^2+{\sigma_{yz}}^2+\sigma_{zx}^2)\right] = \sigma_Y^2 \tag{6.5}$$

6.2 CONSTITUTIVE RELATIONSHIPS IN PLASTICITY

In linear elasticity, stresses and strains are related by Hooke's law:

$$\sigma_{ij} = \lambda e_{kk}\delta_{ij} + 2\mu e_{ij} \tag{6.6}$$

where λ and μ are the Lame constants, δ_{ij} is the Kronecker delta, indices i, j, and k take values 1, 2, and 3 (or x, y, and z), and a repeated index implies summation over the range of the index. This linear relationship between stresses and strains applies

until the yield condition is met. Once the yield criterion is satisfied by stresses, the constitutive law, or the stress–strain relationship, for plasticity should be adopted. Generally speaking, there is no unique stress–strain relationship in plasticity because stresses depend not only on the current strain state, but also on the strain history (note in Figure 6.1 that loading and unloading follow different paths after yielding).

A plasticity consitutive law usually relates the current stress state to strain increments, which is called the flow (or incremental) theory of plasticity. The current strain state is obtained by integrating the strain increments over the entire deformation history. The flow theory is generally used in studies of crack growth wherein unloading occurs near the crack surfaces behind the growing tip. If the material experiences only monotonic and proportional loads, a nonlinear stress–strain relationship may exist. This is the so-called deformation (or total strain) theory, which is generally used in stationary crack problems subjected to monotonically increasing loads.

6.2.1 Flow Theory of Plasticity

A basic assumption in the classical theories of plasticity is that the hydrostatic stress state does not induce plastic deformation, or that the volumetric deformation is purely elastic. The assumption has been confirmed for metals in experiments as long as the deformation is not very severe. Consequently, the volumetric and distorsional deformations can be treated separately in plasticity. First, for linear elastic materials, the relationship between the volumetric strain e_{kk} and the hydrostatic stress σ_{kk} can be obtained from Eq. (6.6) as

$$\sigma_{kk} = 3Ke_{kk} \tag{6.7}$$

Subtracting Eq. (6.7) divided by 3 from Eq. (6.6) yields

$$\sigma'_{ij} = 2\mu e'_{ij} \tag{6.8}$$

where σ'_{ij} and e'_{ij} are the deviatoric stress and strain tensors, respectively, defined by

$$\sigma'_{ij} = \sigma_{ij} - \frac{1}{3}\sigma_{kk}\delta_{ij}, \tag{6.9}$$

$$e'_{ij} = e_{ij} - \frac{1}{3}e_{kk}\delta_{ij} \tag{6.10}$$

and σ'_{ij} and e'_{ij} have only five independent components, respectively, because $\sigma'_{ii} = 0$ and $e'_{ii} = 0$. Equations (6.7) and (6.8) are thus equivalent to Eq. (6.6).

In the flow theory of plasticity, stresses are related to strain increments. The total strain increments consist of the elastic and plastic strain parts, that is,

$$de_{ij} = de^e_{ij} + de^p_{ij} \tag{6.11}$$

According to Hooke's law, in Eqs. (6.7) and (6.8), the elastic strain increments are related to the stress increments by

$$de_{ij}^{e} = \frac{1}{2\mu}\left[d\sigma_{ij} - \frac{\nu}{1+\nu}\delta_{ij}d\sigma_{kk}\right] \tag{6.12}$$

The plastic strain increments are derived from a plastic potential $f(\sigma_{ij})$:

$$de_{ij}^{p} = d\lambda\frac{\partial f}{\partial \sigma_{ij}} \tag{6.13}$$

where $d\lambda$ is a non-negative proportionality factor. The potential $f(\sigma_{ij})$ in the previous equation is often selected as the yield function. Note that the von Mises yield criterion can be expressed in the following form:

$$J_2 - \frac{1}{3}\sigma_Y^2 = 0$$

where J_2 is the second invariant of the deviatoric stress tensor, that is,

$$\begin{aligned} J_2 &= \frac{1}{2}\sigma_{ij}'\sigma_{ij}' \\ &= \frac{1}{6}\left[(\sigma_{xx}-\sigma_{yy})^2 + (\sigma_{yy}-\sigma_{zz})^2 + (\sigma_{zz}-\sigma_{xx})^2 + 6(\sigma_{xy}^2+\sigma_{yz}^2+\sigma_{xz}^2)\right] \end{aligned} \tag{6.14}$$

When using the von Mises yield function as the plastic potential, the constitutive relationship Eq. (6.13) becomes

$$de_{ij}^{p} = d\lambda\frac{\partial J_2}{\partial \sigma_{ij}} = d\lambda\sigma_{ij}' \tag{6.15}$$

which is also called the J_2 flow theory. This constitutive law indicates that

$$\frac{de_{xx}^{p}}{\sigma_{xx}'} = \frac{de_{yy}^{p}}{\sigma_{yy}'} = \frac{de_{zz}^{p}}{\sigma_{zz}'} = \frac{de_{xy}^{p}}{\sigma_{xy}'} = \frac{de_{yz}^{p}}{\sigma_{yz}'} = \frac{de_{xz}^{p}}{\sigma_{xz}'} = d\lambda$$

It is evident from Eq. (6.15) that

$$de_{kk}^{p} = 0$$

Thus, the plastic deformation does not result in volume change.

To obtain the factor $d\lambda$, Eq. (6.15) is self-multiplied to result in

$$de_{ij}^{p}de_{ij}^{p} = d\lambda^2\sigma_{ij}'\sigma_{ij}'$$

We thus have

$$d\lambda = \frac{3\overline{de^p}}{2\overline{\sigma}} \tag{6.16}$$

where $\overline{\sigma}$ is the effective stress defined by

$$\overline{\sigma} = \sqrt{\frac{3}{2}\sigma'_{ij}\sigma'_{ij}} = \sqrt{3J_2} \tag{6.17}$$

and $\overline{de^p}$ is the effective plastic strain increment,

$$\overline{de^p} = \sqrt{\frac{2}{3}de^p_{ij}de^p_{ij}} = \frac{\sqrt{2}}{3}\Big[(de^p_{xx} - de^p_{yy})^2 + (de^p_{yy} - de^p_{zz})^2 + (de^p_{zz} - de^p_{xx})^2 + 6(de^p_{xy})^2 + 6(de^p_{yz})^2 + 6(de^p_{xz})^2\Big]^{1/2} \tag{6.18}$$

Substitution of Eq. (6.16) into Eq. (6.15) yields the plastic strain increments:

$$de^p_{ij} = \frac{3}{2}\frac{\overline{de^p}}{\overline{\sigma}}\sigma'_{ij} \tag{6.19}$$

By substituting the preceding equation and Eq. (6.12) into Eq. (6.11), we obtain the elastic-plastic constitutive relation in the flow theory of plasticity:

$$de_{ij} = \frac{1}{2\mu}\left[d\sigma_{ij} - \frac{\nu}{1+\nu}\delta_{ij}d\sigma_{kk}\right] + \frac{3}{2}\frac{\overline{de^p}}{\overline{\sigma}}\sigma'_{ij} \tag{6.20}$$

This equation gives the strain increments at the current loading state. To obtain the total plastic strains, one needs to integrate Eq. (6.20) over the entire loading history. The effective plastic strain increment in Eq. (6.20) may be expressed as

$$\overline{de^p} = H' d\overline{\sigma}$$

where H' is determined from the uniaxial (x-direction) stress–strain curve for which

$$\overline{\sigma} = \sigma_{xx}, \quad \overline{de^p} = de^p_x$$

It should be noted that the effective stress $\overline{\sigma}$ and effective plastic strain increment $\overline{de^p}$ cannot be independently defined. If $\overline{\sigma}$ is defined first, then the corresponding expression of $\overline{de^p}$ must be derived from the consistency in expressing the plastic work increment, that is,

$$dW^p = \sigma_{ij}de^p_{ij} = \sigma'_{ij}de^p_{ij} = \overline{\sigma}\,\overline{de^p}$$

6.2.2 Deformation Theory of Plasticity

The flow theory Eq. (6.20) applies to materials that undergo plastic deformation under general loading conditions. If the external load produces stress components that increase proportionally, Eq. (6.20) may be simplified to yield a history-independent constitutive law for loading, or the deformation theory, that relates the current state

of stress to the current state of strain. Such a loading is referred to as a proportional loading.

Under proportional loading conditions, stress components vary proportionally, that is,

$$\sigma_{ij} = \tau \sigma_{ij}^{0} \tag{6.21}$$

where τ is a monotonically varying parameter representing loading history and σ_{ij}^{0} are independent of the loading history. Substituting these stresses into Eq. (6.15) yields the plastic strain increments:

$$de_{ij}^{p} = d\lambda \tau \sigma_{ij}^{0\prime}$$

Integrating this equation (over the loading history) leads to

$$e_{ij}^{p} = \phi \sigma_{ij}^{\prime} \tag{6.22}$$

where $\sigma_{ij}^{\prime} = t\sigma_{ij}^{0\prime}$ and

$$\phi = \frac{1}{t} \int \tau d\lambda$$

in which t represents the current loading state. Eq. (6.22) is actually Hencky's assumption on the relationship between plastic strains and stresses.

Self-multiplication of Eq. (6.22) yields

$$e_{ij}^{p} e_{ij}^{p} = \phi^2 \sigma_{ij}^{\prime} \sigma_{ij}^{\prime}$$

We thus obtain the factor ϕ as

$$\phi = \frac{3\overline{e^p}}{2\overline{\sigma}} \tag{6.23}$$

where

$$\overline{e^p} = \sqrt{\frac{2}{3} e_{ij}^{p} e_{ij}^{p}} \tag{6.24}$$

is the effective plastic strain. Note that under proportional deformation conditions,

$$\overline{de^p} = d\overline{e^p}$$

where $\overline{de^p}$ is given in Eq. (6.18). Substituting Eq. (6.23) into Eq. (6.22) yields

$$e_{ij}^{p} = \frac{3\overline{e^p}}{2\overline{\sigma}} \sigma_{ij}^{\prime} \tag{6.25}$$

The final stress–strain relationship in Hencky's deformation theory of plasticity can be written as

$$e'_{ij} = \left(\frac{1}{2\mu} + \frac{3}{2}\frac{\overline{e^p}}{\overline{\sigma}}\right)\sigma'_{ij} \tag{6.26}$$

$$e_{kk} = \frac{1}{3K}\sigma_{kk} \tag{6.27}$$

In Eq. (6.26), the effective plastic strain $\overline{e^p}$ can be related to the effective stress $\overline{\sigma}$ using a single curve assumption according to which the $\overline{e^p}$ versus $\overline{\sigma}$ relation is the same as that in a simple tension test. For the Ramberg-Osgood model, for example,

$$\frac{\overline{e^p}}{e_Y} = \alpha\left(\frac{\overline{\sigma}}{\sigma_Y}\right)^n$$

where α is a constant, $n > 1$ is the hardening exponent, and $e_Y = \sigma_Y/E$ is the yield strain.

6.3 IRWIN'S MODEL FOR MODE I FRACTURE

Irwin [6-1] proposed a stress relaxation model to estimate the plastic zone size ahead of the crack tip. He assumed that the stress distribution outside the plastic zone follows the elastic K-field associated with an adjusted crack length. Within the plastic zone, the stress equals the yield strength of the material. Irwin [6-1] further proposed to use an adjusted stress intensity factor as the fracture driving force for a crack in the presence of small-scale plastic deformation. The plastic deformation effect is taken into account using an effective crack length equal to the physical crack length plus half of the plastic zone size ahead of the crack tip.

6.3.1 Plastic Zone Size

Consider an elastic-perfectly plastic solid with a Mode I crack. To determine the plastic zone size along the crack line (x-axis), we first write down the stresses along the x-axis according to the elastic K-field (see Chapter 3):

$$\begin{aligned}
\sigma_{xx} &= \frac{K_I}{\sqrt{2\pi x}} = \sigma_1 \\
\sigma_{yy} &= \frac{K_I}{\sqrt{2\pi x}} = \sigma_2 \\
\sigma_{zz} = \sigma_3 &= \begin{cases} 0, & \text{plane stress} \\ 2\nu\frac{K_I}{\sqrt{2\pi x}}, & \text{plane strain} \end{cases}
\end{aligned} \tag{6.28}$$

The von Mises yield condition Eq. (6.4) thus becomes on the crack line

$$\sigma_{yy} = \sigma_Y^* \tag{6.29}$$

where σ_Y^* is given by

$$\sigma_Y^* = \begin{cases} \sigma_Y, & \text{plane stress} \\ \frac{1}{1-2\nu}\sigma_Y, & \text{plane strain} \end{cases} \tag{6.30}$$

The condition here indicates that inside the plastic zone and along the x-axis, σ_{yy} must be a constant (σ_Y in plane stress and $\sigma_Y/(1-2\nu)$ in plane strain). If the stress outside the plastic zone were not affected by the yielding, that is, the stress follows Eq. (6.28), the stress distribution would not be able to balance the external load if the upper half of the cracked body is taken as a free body. Hence, the stress must be redistributed outside the plastic zone due to yielding.

A simple method to resolve the problem was suggested by Irwin in which the stress σ_{yy} along the crack line still remains at σ_Y^* within the plastic zone. Outside the plastic zone, σ_{yy} is assumed to follow the K-field Eq. (6.28), but with a fictitious crack tip located at a distance of η from the physical crack tip (Figure 6.2). The fictitious crack tip position must be chosen so that the lost resultant force (represented by area A in Figure 6.2) is equal to the resultant force represented by area B. The effect of the

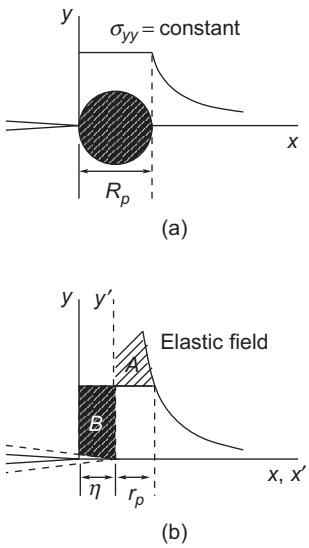

FIGURE 6.2

Irwin's model for estimating plastic zone size. (a) crack tip plastic zone, (b) fictitious crack tip at $x = \eta (x' = 0)$.

elastic-plastic stress field around a crack of length a is thus equivalent to that of an elastic K-field around a crack of length $a+\eta$.

To determine η, we use the condition area A = area B, that is,

$$\int_0^{r_p} \sigma_{yy} dx - \sigma_Y^* r_p = \eta \sigma_Y^* \tag{6.31}$$

where r_p is obtained by substituting Eq. (6.28) into Eq. (6.29):

$$r_p = \frac{1}{2\pi}\left(\frac{K_I}{\sigma_Y^*}\right)^2 \tag{6.32}$$

Integrating Eq. (6.31), we obtain

$$\frac{2K_I}{\sqrt{2\pi}}\sqrt{r_p} - \sigma_Y^* r_p = \eta \sigma_Y^*$$

Hence

$$\eta = r_p$$

Thus, the plastic zone size is given by

$$R_p = r_p + \eta = \frac{1}{\pi}\left(\frac{K_I}{\sigma_Y^*}\right)^2 \tag{6.33}$$

For plane stress, $\sigma_Y^* = \sigma_Y$ and

$$r_p = \frac{K_I^2}{2\pi\sigma_Y^2} \tag{6.34}$$

For plane strain, we have

$$r_p = (1-2\nu)^2 \frac{K_I^2}{2\pi\sigma_Y^2} \tag{6.35}$$

Irwin suggested using

$$r_p = \frac{K_I^2}{6\pi\sigma_Y^2} \tag{6.36}$$

for plane strain, which corresponds to $\nu \approx 0.2$ in Eq. (6.35).

6.3.2 Effective Crack Length and Adjusted Stress Intensity Factor

Irwin's model assumes that the small-scale yielding crack initiation still follows LEFM criterion with an adjusted stress intensity factor due to crack tip plasticity. The adjusted stress intensity factor is obtained using the same formula as in LEFM, but with an effective (half) crack length equal to the physical (half) crack length plus r_p, the half size of the plastic zone, ahead of each crack tip.

Two examples are given here to illustrate the concept. First consider an infinite plate with a crack of length $2a$ subjected to remote stress σ. We know the following stress intensity factor from Chapter 3:

$$\sigma\sqrt{\pi a}$$

Irwin's adjusted stress intensity is thus given by

$$K_I = \sigma\sqrt{\pi a_{eff}} \tag{6.37}$$

where a_{eff} is half the effective crack length defined by

$$a_{eff} = a + r_p \tag{6.38}$$

Substituting Eq. (6.32) into Eqs. (6.38) and (6.37) yields

$$K_I = \sigma\sqrt{\pi\left[a + \frac{1}{2\pi}\left(\frac{K_I}{\sigma_Y^*}\right)^2\right]}$$

Solving for K_I in this equation leads to the adjusted stress intensity factor:

$$K_I = \sigma\sqrt{\pi a}\Big/\sqrt{1 - \frac{1}{2}\left(\frac{\sigma}{\sigma_Y^*}\right)^2} \tag{6.39}$$

The second example involves an edge crack of length a in a semi-infinite plate subjected to remote tension σ. The stress intensity factor expression in LEFM is

$$1.1215\sigma\sqrt{\pi a}$$

The adjusted stress intensity factor now becomes

$$K_I = 1.1215\sigma\sqrt{\pi\left[a + \frac{1}{2\pi}\left(\frac{K_I}{\sigma_Y^*}\right)^2\right]}$$

Solving the previous equation, we have

$$K_I = 1.1215\sigma\sqrt{\pi a}\Big/\sqrt{1 - 0.6289\left(\frac{\sigma}{\sigma_Y^*}\right)^2} \tag{6.40}$$

Due to the simple expressions of the stress intensity factors in the two examples above, the adjusted stress intensity factors are obtained in closed forms. In general, an iteration procedure is needed to obtain the adjusted stress intensity factor. These examples show that the adjusted stress intensity factor reduces to the stress intensity factor in LEFM when $\sigma/\sigma_Y^* << 1$.

6.3.3 Crack Tip Opening Displacement (CTOD)

With Irwin's plastic zone model, we can define the crack opening displacement at the physical crack tip. According to Irwin's model, the physical crack tip lies on the elastic-plastic boundary and thus, the elastic solution associated with the fictitious crack tip is valid at the point. The crack opening displacement field is now given by

$$2u_y = \frac{8K_I}{E^*}\sqrt{\frac{r}{2\pi}}$$

where r is the distance from the fictitious crack tip. The CTOD, δ, is defined as

$$\delta = 2u_y\big|_{r=r_p}$$

Substituting r_p from Eq. (6.32) into the preceding equation, we obtain the CTOD in Irwin's model:

$$\delta = \frac{4}{\pi E^*}\frac{K_I^2}{\sigma_Y^*} = \frac{4G_I}{\pi\sigma_Y^*} \tag{6.41}$$

The CTOD now is proportional to the square of stress intensity factor.

6.4 THE DUGDALE MODEL

Due to the nonlinear and history-dependent nature of plasticity, it is often necessary to use simplified models to treat elastic-plastic fracture problems, for example, Irwin's model in the previous section. The Dugdale model represents another commonly used model in elastic-plastic fracture mechanics. In the Dugdale model [6-2], yielding is assumed to occur only in a narrow strip zone with zero height along the crack line. This strip yield zone is then treated as an extended part of the physical crack with the closure yield stress acting on the extended crack faces. The strip yield zone and the physical crack form the effective crack. With the Dugdale model, the elastic-plastic crack problem is reduced to an elastic one with finite stresses at the effective crack tip, which is actually a point on the elastic-plastic boundary. The Dugdale model is first introduced for small-scale yielding Mode I cracks, and is subsequently described for a centrally cracked infinite plate.

6.4.1 Small-Scale Yielding

Figure 6.3 shows a strip yield zone with a length of R_0 ahead of a crack tip. The yield zone is treated as a part of the effective crack in the Dugdale model. The applied load thus induces a stress intensity factor at the effective crack tip. Here we do not distinguish this stress intensity factor with that at the physical crack tip, that is,

$$K_I(a+R_0) = K_I(a)$$

where a is the physical crack length, because $R_0 << a$ according to small-scale yielding.

According to the Dugdale model, stresses are finite at the effective crack tip. Because the stress singularity is associated with the stress intensity factor, this finite stress condition can be met if and only if K_I due to the external loading is negated by $K_I^{(2)}$ induced by the yield stress along the strip yield zone, that is,

$$K_I + K_I^{(2)} = 0 \tag{6.42}$$

To calculate $K_I^{(2)}$, we use the known solution for a pair of concentrated forces P applied on the crack faces at a distance η from the effective crack tip as shown in Figure 6.4:

$$K_I^P = \frac{\sqrt{2}P}{\sqrt{\pi\eta}}$$

For the distributed traction σ_Y^* acting on the crack faces from $\eta = 0$ at the effective crack tip to $\eta = R_0$ at the physical crack tip, the stress intensity may be obtained by replacing P in the equation with $-\sigma_Y^* d\eta$ and integrating from $\eta = 0$ to $\eta = R_0$ as

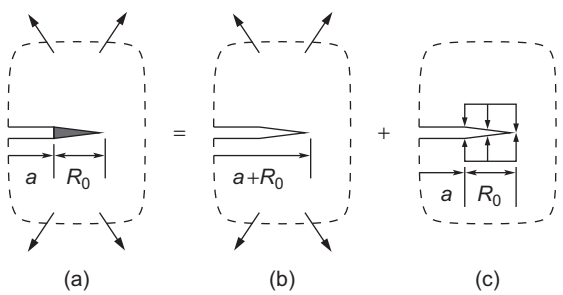

FIGURE 6.3

Dugdale yield zone in small-scale yielding.

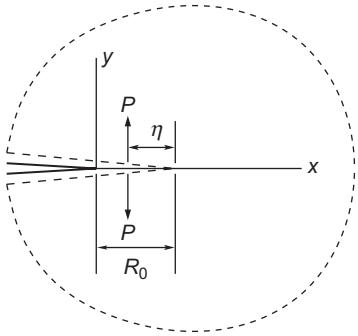

FIGURE 6.4

A pair of concentrated forces exerted on the crack faces.

follows:

$$K_I^{(2)} = \int_0^{R_0} \frac{-\sqrt{2}\sigma_Y^* d\eta}{\sqrt{\pi\eta}}$$

$$= -2\sigma_Y^* \sqrt{\frac{2R_0}{\pi}}$$

Substituting this expression into Eq. (6.42) yields

$$2\sigma_Y^* \sqrt{\frac{2R_0}{\pi}} = K_I$$

We thus obtain the length of the plastic zone,

$$R_0 = \frac{\pi}{8}\left(\frac{K_I}{\sigma_Y^*}\right)^2 \tag{6.43}$$

For plane stress, $\sigma_Y^* = \sigma_Y$,

$$R_0 \simeq 0.392\left(\frac{K_I}{\sigma_Y}\right)^2$$

This compares to the plastic zone size of Irwin's model,

$$R_p = \frac{1}{\pi}\left(\frac{K_I}{\sigma_Y}\right)^2 \simeq 0.318\left(\frac{K_I}{\sigma_Y}\right)^2$$

The opening displacement at the physical crack tip (CTOD) as a result of the applied stress intensity can be obtained from the crack tip displacement expression

in Chapter 3:

$$\delta^{(1)} = \frac{8K_I}{E^*}\sqrt{\frac{r}{2\pi}}\bigg|_{r=R_0} = \frac{2K_I^2}{E^*\sigma_Y^*}$$

The crack opening displacement due to a pair of concentrated forces P as shown in Figure 6.4 can be obtained from the Westergaard function given in Problem 3.6 as

$$\delta^{(2)} = \frac{4P}{\pi E^*}\ln\left|\frac{\sqrt{|R_0 - x|} + \sqrt{\eta}}{\sqrt{|R_0 - x|} - \sqrt{\eta}}\right|$$

At the physical crack tip $r = R_0$, the CTOD due to the yield stress in the plastic zone is obtained by taking $P = \sigma_Y^* d\eta$ in the previous equation and then integrating over the plastic zone, that is,

$$\begin{aligned}\delta^{(2)} &= -\frac{4\sigma_Y^*}{\pi E^*}\int_0^{R_0}\ln\frac{\sqrt{R_0} + \sqrt{\eta}}{\sqrt{R_0} - \sqrt{\eta}}d\eta \\ &= -\frac{K_I^2}{E^*\sigma_Y^*}\end{aligned}$$

The total CTOD at the physical crack tip is thus obtained as follows:

$$\begin{aligned}\delta &= \delta^{(1)} + \delta^{(2)} \\ &= \frac{K_I^2}{E^*\sigma_Y^*}\end{aligned} \tag{6.44}$$

This value is slightly smaller than the CTOD in Irwin's model Eq. (6.41).

6.4.2 A Crack in an Infinite Plate

Unlike Irwin's model, which is restricted to small-scale yielding, the Dugdale model also applies to large-scale yielding cases. We now consider an infinite plate with a crack of length $2a$ subjected to remote tensile stress σ, as shown in Figure 6.5. Now the effective crack has a length of $2(a + R_0)$, where R_0 is the length of the strip yield zone.

We still use the superposition method to treat the problem. The stress intensity factor at the tip of the effective crack due to the remote tension is

$$K_I = \sigma\sqrt{\pi(a + R_0)}$$

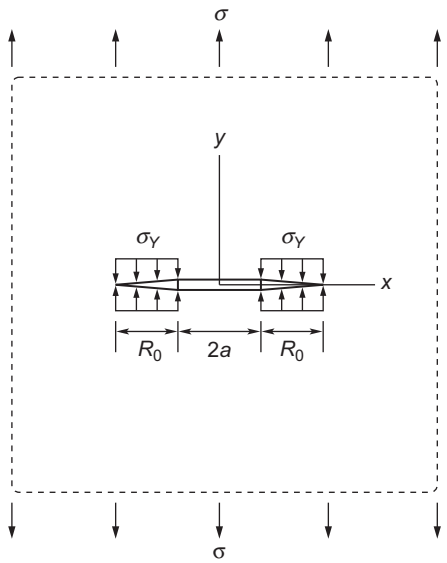

FIGURE 6.5

Dugdale yield zones ahead of crack tips in an infinite plate subjected to tension.

For the stress to remain finite at the effective crack tip, K_I should be negated by the following stress intensity factor due to the yield stress in the strip yield zone:

$$K_I^{(2)} = -2\sigma_Y^* \sqrt{\frac{a+R_0}{\pi}} \int_a^{a+R_0} \frac{d\eta}{(a+R_0)^2 - \eta^2}$$

$$= -2\sigma_Y^* \sqrt{\frac{a+R_0}{\pi}} \cos^{-1}\left(\frac{a}{a+R_0}\right)$$

The cancellation of stress singularity at the effective crack tip thus requires

$$\sigma\sqrt{\pi(a+R_0)} - 2\sigma_Y^* \sqrt{\frac{a+R_0}{\pi}} \cos^{-1}\left(\frac{a}{a+R_0}\right) = 0$$

The yield zone length is obtained from this equation:

$$\frac{R_0}{a} = \sec\left(\frac{\pi\sigma}{2\sigma_Y^*}\right) - 1 \tag{6.45}$$

Now calculate the CTOD at the physical crack tip, or the tail of the yield zone. The CTOD due to the remote tension is

$$\delta^{(1)} = \frac{4\sigma}{4E^*}\sqrt{(a+R_0)^2 - a^2}$$

This CTOD is reduced by that due to the yield stress:

$$\delta^{(2)} = -\frac{8\sigma_Y^*}{\pi E^*}\sqrt{(a+R_0)^2 - a^2}\cos^{-1}\left(\frac{a}{a+R_0}\right)$$

The total CTOD at the physical crack tip is thus obtained as

$$\begin{aligned}\delta &= \delta^{(1)} + \delta^{(2)} \\ &= \frac{8a\sigma_Y^*}{\pi E^*}\ln\left(\sec\frac{\pi\sigma}{2\sigma_Y^*}\right)\end{aligned} \tag{6.46}$$

Equations (6.45) and (6.46) are valid for load levels up to $\sigma = \sigma_Y^*$, which corresponds to the failure of comprehensive yielding. In this case, the failure is no longer characterized by crack growth. In general, the crack will grow before σ reaches σ_Y^*. To study the yielding effect at small ratio of σ/σ_Y^*, Eqs. (6.45) and (6.46) are expanded into Taylor series as follows:

$$\frac{R_0}{a} = \frac{1}{2}\left(\frac{\pi\sigma}{2\sigma_Y^*}\right)^2 + \frac{5}{24}\left(\frac{\pi\sigma}{2\sigma_Y^*}\right)^4 + \cdots$$

$$\delta = \frac{8a\sigma_Y^*}{\pi E^*}\left[\frac{1}{2}\left(\frac{\pi\sigma}{2\sigma_Y^*}\right)^2 + \frac{1}{12}\left(\frac{\pi\sigma}{2\sigma_Y^*}\right)^4 + \cdots\right]$$

When $\sigma/\sigma_Y^* << 1$, this series can be approximated by

$$R_0 = \frac{\pi}{8}\left(\frac{K_I}{\sigma_Y^*}\right)^2 \tag{6.47}$$

$$\delta = \frac{K_I^2}{E^*\sigma_Y^*} \tag{6.48}$$

Here we have employed $K_I = \sigma\sqrt{\pi a}$ because $R_0 << a$. The preceding results about the plastic zone size and CTOD agree with the small-scale-yielding results Eqs. (6.43) and (6.44), respectively.

In general, the Dugdale model predicts crack growth based on a CTOD criterion. This will be discussed in Chapter 7. For small-scale yielding, Eqs. (6.44) and (6.48) can be rewritten as

$$K_I = \sqrt{E^*\sigma_Y^*\delta} \tag{6.49}$$

which is theoretically valid when the applied stress is much smaller than the yield stress. Burdekin and Stone [6-3] suggested using Eq. (6.49) for moderately higher load level. Thus, an LEFM approach may be combined with the Dugdale model to predict fracture.

6.5 PLASTIC ZONE SHAPE ESTIMATE ACCORDING TO THE ELASTIC SOLUTION

Knowledge of the plastic zone shape and size around a crack is useful to understanding the plasticity effect on the fracture behavior of solids. In general, complete solutions of stresses in both elastic and plastic regions are needed to determine the plastic zone shape. If the plastic zone around the crack tip is small compared to the region in which the crack tip K-fields apply, the singular elastic stress fields may be used to estimate the plastic zone shape. The estimates thus obtained, however, are the first-order approximations because the stress redistribution caused by the small plastic zone is not considered. In the following part of this section, the plastic zone shapes are estimated for Mode I cracks in both plane stress and plane strain fields. Mode II loading cases can be treated in a similar manner.

6.5.1 Principal Stresses

Use of the Tresca yield condition to determine the plastic zone requires principal stress information. We thus first determine the principal stresses based on the near-tip elastic stress fields. Under Mode I loading conditions, the K-field around the crack tip is given by

$$\begin{aligned}
\sigma_{xx} &= \frac{K_I}{\sqrt{2\pi r}}\left[1-\sin\frac{\theta}{2}\sin\frac{3\theta}{2}\right]\cos\frac{\theta}{2}\\
\sigma_{yy} &= \frac{K_I}{\sqrt{2\pi r}}\left[1+\sin\frac{\theta}{2}\sin\frac{3\theta}{2}\right]\cos\frac{\theta}{2}\\
\sigma_{xy} &= \frac{K_I}{\sqrt{2\pi r}}\sin\frac{\theta}{2}\cos\frac{\theta}{2}\cos\frac{3\theta}{2}\\
\sigma_{zz} &= \begin{cases} 0, & \text{plane stress}\\ \nu(\sigma_{xx}+\sigma_{yy}), & \text{plane strain}\end{cases}
\end{aligned} \tag{6.50}$$

Since $\sigma_{yz}=\sigma_{xz}=0$, $\sigma_{zz}=\sigma_3$ is a principal stress. The other two principal stresses in the $x-y$ plane are given by

$$\left.\begin{matrix}\sigma_1\\ \sigma_2\end{matrix}\right\} = \frac{1}{2}(\sigma_{xx}+\sigma_{yy}) \pm \sqrt{\frac{1}{4}(\sigma_{xx}-\sigma_{yy})^2+\sigma_{xy}^2}$$

Substitution of Eq. (6.50) into these expressions yields

$$\begin{aligned}\sigma_1 &= \frac{K_I}{\sqrt{2\pi r}}\cos\frac{\theta}{2}\left[1+\sin\frac{\theta}{2}\right]\\ \sigma_2 &= \frac{K_I}{\sqrt{2\pi r}}\cos\frac{\theta}{2}\left[1-\sin\frac{\theta}{2}\right]\end{aligned} \tag{6.51}$$

Similarly, we have the principle stress σ_3,

$$\sigma_3 = \begin{cases} 0, & \text{plane stress} \\ 2\nu\frac{K_I}{\sqrt{2\pi r}}\cos\frac{\theta}{2}, & \text{plane strain}\end{cases} \tag{6.52}$$

6.5.2 Plane Stress Case

In the following, both Tresca and Mises yield criteria are used to estimate the crack tip plastic zone shape and size for plane stress. It can be seen that the two criteria result in different plastic zone shapes but the same plastic zone size ahead of the crack.

Plastic Zone Estimate Based on the Tresca Yield Criterion

Equations (6.51) and (6.52) indicate that $\sigma_1 \geq \sigma_2 \geq \sigma_3$ for plane stress when $\theta \geq 0$. The Tresca yield criterion Eqs. (6.1) and (6.2) now reduces to

$$\sigma_1 - \sigma_3 = \sigma_Y \tag{6.53}$$

Substitution of Eqs. (6.51) and (6.52) into this equation leads to

$$\frac{K_I}{\sqrt{2\pi r}}\left[1+\sin\frac{\theta}{2}\right]\cos\frac{\theta}{2} = \sigma_Y$$

The elastic-plastic boundary is obtained by solving this equation for r as follows:

$$r = \frac{K_I^2}{2\pi\sigma_Y^2}\cos^2\frac{\theta}{2}\left[1+\sin\frac{\theta}{2}\right]^2, \qquad \theta \geq 0 \tag{6.54}$$

Figure 6.6 depicts the elastic-plastic boundary represented by this expression. Here the boundary for $\theta < 0$ is obtained by symmetry.

Plastic Zone Estimate Based on the von Mises Yield Criterion

Substituting Eqs. (6.51) and (6.52) into the von Mises criterion Eq. (6.4), we obtain the elastic-plastic boundary as follows:

$$r = \frac{K_I^2}{2\pi\sigma_Y^2}\cos^2\frac{\theta}{2}\left[1+3\sin^2\frac{\theta}{2}\right] \tag{6.55}$$

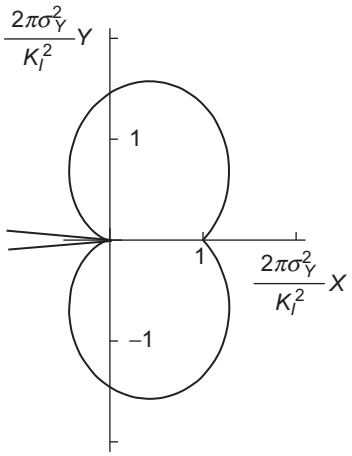

FIGURE 6.6

Plastic zone shape estimate based on the Tresca criterion in plane stress.

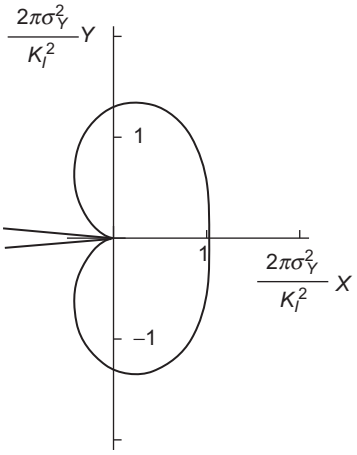

FIGURE 6.7

Plastic zone shape estimate based on the von Mises criterion in plane stress.

A plot of this expression is shown in Figure 6.7. The plastic zone size along the crack line ($\theta = 0$) is

$$R_p = r(\theta = 0) = \frac{1}{2\pi}\left(\frac{K_I}{\sigma_Y}\right)^2$$

which is half of Irwin's estimate Eq. (6.33).

6.5.3 Plane Strain Case

The Tresca and Mises yield conditions are again used to approximately determine the crack tip plastic zone shape and size for plane strain. We will see that the plastic zone size for plane strain is much smaller than that for the corresponding plane stress case.

Plastic Zone Estimate Based on the Tresca Yield Criterion

In the plane strain case, application of the Tresca yield criterion depends on Poisson's ratio because it influences the magnitude of σ_3 relative to σ_2. Since σ_3 can be expressed as

$$\sigma_3 = \nu(\sigma_1 + \sigma_2)$$

it is easy to show that when $\theta \geq 0$,

$$\sigma_1 \geq \sigma_2 \geq \sigma_3, \quad \text{if} \quad \nu \leq \frac{\sigma_2}{\sigma_1 + \sigma_2} \tag{6.56}$$

and

$$\sigma_1 \geq \sigma_3 \geq \sigma_2, \quad \text{if} \quad \nu \geq \frac{\sigma_2}{\sigma_1 + \sigma_2} \tag{6.57}$$

The corresponding functions of the elastic-plastic boundary are ($\theta \geq 0$)

$$r = \frac{K_I^2}{2\pi\sigma_Y^2}\cos^2\frac{\theta}{2}\left(1 - 2\nu + \sin\frac{\theta}{2}\right)^2, \quad \nu \leq \frac{\sigma_2}{\sigma_1 + \sigma_2} \tag{6.58}$$

$$r = \frac{K_I^2}{2\pi\sigma_Y^2}\sin^2\theta, \quad \nu \geq \frac{\sigma_2}{\sigma_1 + \sigma_2} \tag{6.59}$$

respectively. The contour of the plastic zone is to be constructed from these two functions depending on the inequalities in Eqs. (6.56) and (6.57). For $\nu = 1/2$, Eq. (6.57) is always satisfied. Hence, the plastic zone contour is given by Eq. (6.59) and is depicted in Figure 6.8. Again the boundary for $\theta < 0$ is obtained by symmetry.

Plastic Zone Estimates Based on the von Mises Yield Criterion

The plastic zone boundary according to the von Mises yield criterion Eq. (6.4) is obtained by substituting Eqs. (6.51) and (6.52) into Eq. (6.4):

$$r = \frac{K_I^2}{2\pi\sigma_Y^2}\cos^2\frac{\theta}{2}\left[(1 - 2\nu)^2 + 3\sin^2\frac{\theta}{2}\right] \tag{6.60}$$

This function indicates that the plastic zone shape in plane strain depends on Poisson's ratio (this is also the case with the Tresca yielding condition; see Eqs. (6.58) and (6.59)). The reason is that Poisson's ratio affects the stress triaxiality, which

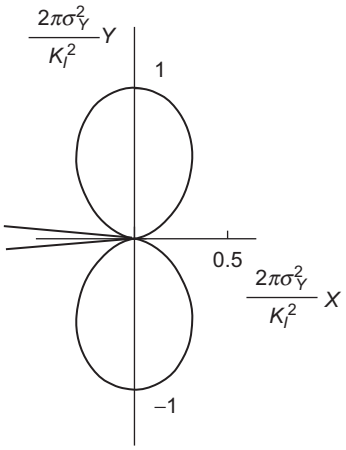

FIGURE 6.8

Plastic zone shape estimate based on the Tresca criterion in plane strain ($\nu = 1/2$).

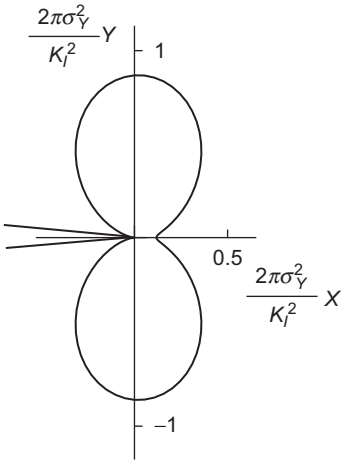

FIGURE 6.9

Plastic zone shape estimate based on the von Mises criterion in plane strain ($\nu = 0.3$).

restricts the plastic deformation. For example, the plastic zone size ahead of the crack tip ($\theta = 0^o$) is given by

$$R_p = r(\theta = 0) = \frac{K_I^2}{2\pi\sigma_Y^2}, \quad \text{if } \nu = 0$$

$$R_p = r(\theta = 0) = 0, \quad \text{if } \nu = 0.5$$

Figure 6.9 depicts the plastic zone shape according to Eq. (6.60) for $\nu = 0.3$.

A comparison of the plastic zone size along the crack line between plane stress Eq. (6.55) and plane strain Eq. (6.60) ($\nu = 0.3$) using the von Mises condition shows that the plane strain value of

$$R_p = r(\theta = 0) = \frac{0.16}{2\pi}\left(\frac{K_I}{\sigma_Y}\right)^2$$

is only 16% of the corresponding plane stress value,

$$R_p = r(\theta = 0) = \frac{1}{2\pi}\left(\frac{K_I}{\sigma_Y}\right)^2$$

for the same applied K_I. The smaller plastic zone size in plane strain results from the triaxiality of the stress state, which restricts plastic yielding.

6.5.4 Antiplane Strain Case

The plastic zone shape for anti-plane strain, or Mode III case using the elastic K-field is introduced. The result obtained can be compared with that of the complete small-scale yielding solution in Section 6.7. The stresses in the Mode III elastic K-fields are

$$\sigma_{yz} = \frac{K_{III}}{\sqrt{2\pi r}}\cos\frac{1}{2}\theta$$

$$\sigma_{xz} = -\frac{K_{III}}{\sqrt{2\pi r}}\sin\frac{1}{2}\theta$$

Substitution of these stresses into the von Mises yield criterion Eq. (6.5) yields

$$\frac{K_{III}^2}{2\pi r} = \frac{1}{3}\sigma_Y^2$$

Thus, the plastic zone boundary is described by a circle of radius

$$r_p = \frac{3K_{III}^2}{2\pi\sigma_Y^2} \tag{6.61}$$

with the center located at the crack tip. It is of interest to note that the plastic zone in the small-scale yielding solution in Section 6.7 is also a circle with the same radius r_p in Eq. (6.61), but centered at $x = r_p$ along the crack line. The plastic zone size along the crack line is thus twice that given in Eq. (6.61).

6.6 PLASTIC ZONE SHAPE ACCORDING TO FINITE ELEMENT ANALYSES

The plastic zone shapes and sizes estimated from the elastic singular stress field introduced in the previous section are only the first-order approximations. The estimated plastic zone tends to be smaller than the actual size. For example, the plastic zone size given in Eq. (6.55) for plane stress is only half of Irwin's estimate, which is believed to be closer to the actual size. A more realistic estimate of plastic zone shape and size can be made by elastic-plastic finite element analyses. This section introduces the numerical results in Kim [6-4].

Figure 6.10 shows the near-tip plastic zone shapes and sizes for a centrally cracked plate under plane stress conditions using both the K-field and the finite element analysis. The plate is subjected to a tensile load as shown and the crack length is much smaller than the in-plane specimen size (the width of the plate is 10 times the crack length in the calculation). The von Mises yield criterion is used in the calculations. Poisson's ratio is taken as 0.3. For ease of comparison, all the sizes are normalized with respect to that of the elastic solution for the load level of $K_I/(\sigma_Y\sqrt{\pi a}) = 0.3$. It is seen that the plastic zone size on the crack line by the K-field estimate is about half of the finite element solution when the applied stress level $K_I/(\sigma_Y\sqrt{\pi a}) = 0.4$. The difference of the plastic zone size along the y-direction is moderate at this load level.

Figure 6.11 shows the near-tip plastic zones for the plane strain case. It is seen that the plastic zone size on the crack line by the K-field estimate closely matches that by the finite element analysis although the K-field estimate in the y-direction is significantly smaller than that of the numerical analysis even at a load level of $K_I/(\sigma_Y\sqrt{\pi a}) = 0.2$. The plastic zone size along the crack line is less than 5% of the crack length, indicating small-scale yielding prevails at this load level.

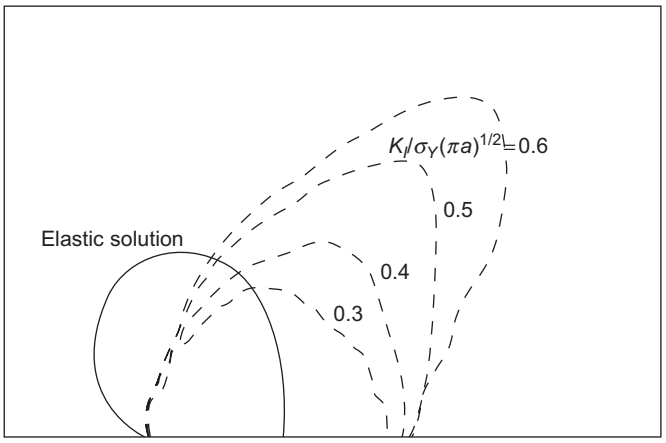

FIGURE 6.10

Plane stress crack tip plastic zone by finite element analyses (adapted from Kim [6-4]).

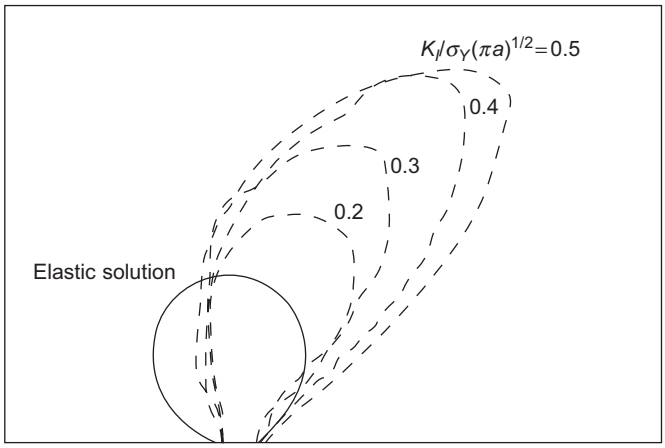

FIGURE 6.11

Plane strain crack tip plastic zone by finite element analysis (adapted from Kim [6-4]).

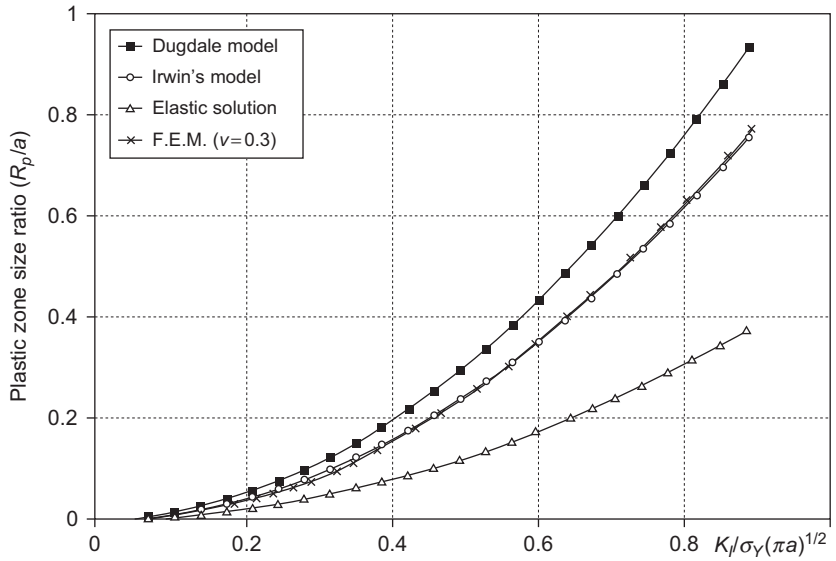

FIGURE 6.12

Plane stress plastic zone size along the crack line for a centrally cracked plate (adapted from Kim [6-4]).

Figure 6.12 further shows the plane stress plastic zone size estimates versus the loading parameter $K_I/(\sigma_Y\sqrt{\pi a})$ along the crack line using the elastic K-field solution, the Dugdale model (based on small-scale yielding), Irwin's model, and the finite element analysis. The plastic zone size is normalized by the half crack length a. It is

observed that the plastic zone size predicted from Irwin's model agrees very well with the numerical results. While the K-field solution significantly underestimates the plastic zone size, the Dugdale model generally overestimates the plastic zone size. For the plane strain case, Irwin's prediction is not as good as in the plane stress case, while the elastic solution seems to be quite accurate up to $K_I/(\sigma_Y\sqrt{\pi a}) = 0.5$.

6.7 A MODE III SMALL-SCALE YIELDING SOLUTION

The nonlinearity of the elastic-plastic constitutive relationship makes it extremely difficult to obtain closed-form solutions for elastic-plastic crack problems, especially the in-plane Mode I or Mode II problems. For Mode III crack problems, however, closed-form solutions may be obtained under small-scale yielding conditions. The significance of the Mode III small-scale yielding solution lies in the fact that Irwin's assumption on the elastic field around a Mode I crack in an elastic-perfectly plastic material agrees with the Mode III solution.

This offers some support for Irwin's adjusted stress intensity factor approach based on the effective crack length, which has proven convenient and effective in predicting fracture of metals under small-scale yielding conditions. In this section, the small-scale yielding solution is introduced for an elastic-perfectly plastic material studied by Hult and McClintock [6-5].

6.7.1 Basic Equations

We know from Chapter 3 that, under Mode III deformation conditions, there are only five nonzero field quantities independent of the coordinate z, that is,

$$\begin{aligned} \tau_x &= \sigma_{xz}, \quad & \tau_y &= \sigma_{yz} \\ \gamma_x &= 2e_{xz}, \quad & \gamma_y &= 2e_{yz} \\ w &= u_z \end{aligned}$$

Figure 6.13 shows the coordinate systems used in the study.

The anti-plane shear stresses satisfy the equilibrium equation:

$$\frac{\partial \tau_x}{\partial x} + \frac{\partial \tau_y}{\partial y} = 0 \tag{6.62}$$

The anti-plane shear strains and the out-of-plane displacement are related by

$$(\gamma_x, \gamma_y) = \left(\frac{\partial w}{\partial x}, \frac{\partial w}{\partial y}\right) \tag{6.63}$$

In the elastic region, the preceding equations are supplemented by Hooke's law:

$$(\gamma_x, \gamma_y) = \frac{1}{\mu}(\tau_x, \tau_y) \tag{6.64}$$

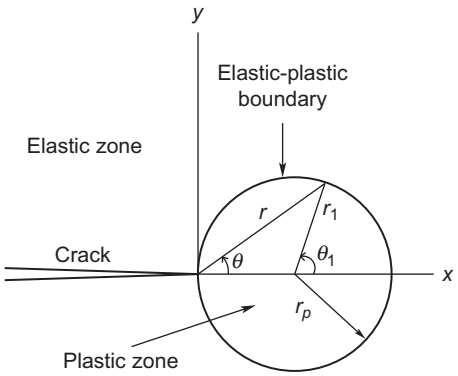

FIGURE 6.13

Plastic zone ahead of a Mode III crack in an elastic-perfectly plastic material in small-scale yielding and coordinate systems.

which is reduced from Eq. (6.6). We thus have five equations in Eqs. (6.62) through (6.64) for the two stresses, two strains, and the displacement.

In the plastic zone, the von Mises yield condition Eq. (6.5) reduces to

$$\tau_x^2 + \tau_y^2 = \tau_Y^2 \tag{6.65}$$

where $\tau_Y = \sigma_Y/\sqrt{3}$ is the yield stress in shear. The constitutive relationship of the deformation plasticity, Eqs. (6.26) and (6.27), now reduces to

$$(\gamma_x, \gamma_y) = \lambda\,(\tau_x, \tau_y) \tag{6.66}$$

where λ is a proportionality factor. Now we have six equations in Eqs. (6.62), (6.63), (6.65), and (6.66) for the two stresses, two strains, the displacement, and the factor λ.

6.7.2 Elastic-Plastic Solution and the Crack Tip Plastic Zone

In the plastic zone, the yield condition Eq. (6.65) indicates that the stress vector (τ_x, τ_y) has a constant magnitude. It can be easily verified that the stresses

$$\tau_x = -\tau_Y \sin\theta, \quad \tau_y = \tau_Y \cos\theta \tag{6.67}$$

satisfy the equilibrium equation (6.62) and the yield condition Eq. (6.65), where θ is a polar coordinate defined by

$$x = r\cos\theta, \quad y = r\sin\theta \tag{6.68}$$

Substituting the stresses Eq. (6.67) into the constitutive relationship Eq. (6.66) yields the following strains:

$$\gamma_x = -\lambda\tau_Y \sin\theta, \quad \gamma_y = \lambda\tau_Y \cos\theta$$

Using these strain expressions and the strain-displacement relations in Eq. (6.63), we can arrive at

$$dw = \gamma_x dx + \gamma_y dy = 0$$

along $\theta = \text{const.}$ ($d\theta = 0$). Hence, the displacement w is a function of θ only, that is,

$$w = F(\theta) \tag{6.69}$$

where $F(\theta)$ is an unknown function to be determined. Use of the displacement above and the strain-displacement relations in the polar coordinates (r,θ) yields the following strains in the polar coordinate system:

$$\gamma_r = \frac{\partial w}{\partial r} = 0, \quad \gamma_\theta = \frac{1}{r}\frac{\partial w}{\partial \theta} = \frac{1}{r}\frac{dF(\theta)}{d\theta} \tag{6.70}$$

It can be seen from Eq. (6.67) that the stresses in the plastic zone do not satisfy the traction-free boundary condition $\tau_y = 0$ on the crack face ($y = 0, x < 0$, or $\theta = \pm\pi$). The plastic zone thus does not contain the crack surfaces. In the small-scale yielding problem, we assume that the yield zone around the crack tip is so small that the elastic K-field is not disturbed at distances far away from the yield zone. Mathematically, this condition can be described by (see Chapter 3 for the Mode III K-field)

$$\tau_y + i\tau_x \to \frac{K_{III}}{\sqrt{2\pi z}}, \quad |z|/r_p \to \infty \tag{6.71}$$

where K_{III} is the Mode III stress intensity factor, $2r_p$ is the yield zone size, and $z = x + iy$ is the complex coordinate. The asymptotic condition at $|z|/r_p \to \infty$ means that we can consider a semi-infinite plane (after symmetry consideration) for the small-scale yielding crack problem, as shown in Figure 6.14.

Outside the plastic zone, we consider the following elastic stresses:

$$\tau_y + i\tau_x = \frac{K_{III}}{\sqrt{2\pi z_1}} = \frac{K_{III}}{\sqrt{2\pi (z - r_p)}} \tag{6.72}$$

where $z_1 = z - r_p$, with r_p being the half plastic zone size along the crack line. The preceding solution clearly satisfies the asymptotic condition Eq. (6.71) and also the crack face traction-free condition because $z_1 \to z$ when $|z|/r_p \to \infty$.

In the following, the stress and displacement continuity conditions are employed to determine the plastic zone shape and size, as well as the function $F(\theta)$ in the

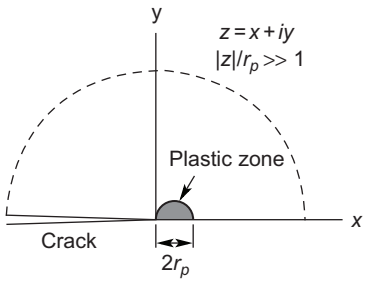

FIGURE 6.14

Small-scale yielding in the physical plane.

displacement Eq. (6.69). First, the elastic stress field Eq. (6.72) and the corresponding displacement are rewritten in polar coordinates (r_1, θ_1) as follows:

$$(\tau_x, \tau_y) = \frac{K_{III}}{\sqrt{2\pi r_1}}\left(-\sin\frac{\theta_1}{2}, \cos\frac{\theta_1}{2}\right)$$

$$w = \frac{K_{III}}{\mu}\sqrt{\frac{2r_1}{\pi}}\sin\frac{\theta_1}{2}$$

where (r_1, θ_1) is defined by (see Figure 6.13)

$$z_1 = z - r_p = r_1(\cos\theta_1 + i\sin\theta_1)$$

Use of the stress and displacement continuity conditions at the elastic-plastic boundary yields the following equations to determine the function $F(\theta)$, r_1, and the relation between θ_1 and θ:

$$\begin{aligned}
\tau_Y \sin\theta &= \frac{K_{III}}{\sqrt{2\pi r_1}}\sin\frac{\theta_1}{2} \\
\tau_Y \cos\theta &= \frac{K_{III}}{\sqrt{2\pi r_1}}\cos\frac{\theta_1}{2} \\
F(\theta) &= \frac{K_{III}}{\mu}\sqrt{\frac{2r_1}{\pi}}\sin\frac{\theta_1}{2}
\end{aligned} \tag{6.73}$$

r_1 and θ_1 can be obtained from the first two equations in Eq. (6.73) as follows:

$$r_1 = \frac{1}{2\pi}\left(\frac{K_{III}}{\tau_Y}\right)^2 \tag{6.74}$$

$$\theta_1 = 2\theta \tag{6.75}$$

Hence, the elastic-plastic boundary is a circle with a radius

$$r_p = \frac{1}{2\pi}\left(\frac{K_{III}}{\tau_Y}\right)^2 \tag{6.76}$$

and centered at $(x,y) = (r_p, 0)$, as shown in Figure 6.13.

The function $F(\theta)$, and hence the displacement w in the plastic zone according to Eq. (6.69), can be obtained from the last equation in Eq. (6.73) as follows:

$$w = F(\theta) = \frac{\gamma_Y K_{III}^2}{\pi \tau_Y^2}\sin\theta \tag{6.77}$$

where $\gamma_Y = \tau_Y/\mu$ is the yield strain in shear. Substituting the displacement above into Eq. (6.70), we have the strain components in the plastic zone:

$$\gamma_r = 0, \quad \gamma_\theta = \frac{\gamma_Y K_{III}^2}{\pi \tau_Y^2}\frac{\cos\theta}{r} \tag{6.78}$$

In elastic-plastic fracture mechanics, the CTOD is often used as a fracture parameter. The CTOD, or δ, for the Mode III small-scale yielding problem is obtained using Eq. (6.77) as follows:

$$\begin{aligned}\delta &= w|_{\theta=\pi/2} - w|_{\theta=-\pi/2} \\ &= \frac{2\gamma_Y}{\pi}\left(\frac{K_{III}}{\tau_Y}\right)^2\end{aligned} \tag{6.79}$$

Some important conclusions can be made from the small-scale yielding solution for the elastic-perfectly plastic material as follows:

1. The plastic zone has a circular shape with a diameter of $(K_{III}/\tau_Y)^2/\pi$ ahead of the crack tip.
2. The stresses are finite and the strains are singular at the crack tip, $r = 0$, with an order of $1/r$ versus $1/\sqrt{r}$ in the linear elastic case.
3. The stresses and displacement in the elastic zone are identical to those in LEFM with the crack tip located at the center of the plastic zone.

The last result is particularly significant because Irwin's adjusted stress intensity factor approach based on the effective crack length agrees with this Mode III solution.

6.8 A MODE III SMALL-SCALE YIELDING SOLUTION—ELASTIC POWER-LAW HARDENING MATERIALS

In the previous section, we introduced the Mode III stress and deformation solutions for a crack in an elastic perfectly plastic material under small-scale yielding (SSY)

conditions. Metallic materials usually exhibit strain-hardening behavior. The stress–strain relation for strain-hardening materials may be appropriately described by the power law. This section thus introduces the SSY solution for a Mode III crack in an elastic power-law hardening material obtained by Rice [6-9].

6.8.1 Basic Equations

For elastic power-law hardening materials, the equilibrium equation is still given by Eq. (6.62) and the strain-displacement relations are given by Eq. (6.63). In the hardening material case, we often use the strain compatibility condition by eliminating w in Eq. (6.63) as follows

$$\frac{\partial \gamma_y}{\partial x} - \frac{\partial \gamma_x}{\partial y} = 0 \tag{6.80}$$

In the elastic region, the preceding equations are supplemented by Hooke's law (6.64). We thus have four equations in Eqs. (6.62), (6.80), and (6.64) for the two stresses and two strains. The displacement can be obtained from the strain-displacement relations (6.63) upon solving for the strains.

In the plastic zone characterized by

$$\tau = \sqrt{\tau_x^2 + \tau_y^2} \geq \tau_Y \tag{6.81}$$

the constitutive relationship of the deformation plasticity, Eq. (6.26), reduces to

$$(\gamma_x, \gamma_y) = \frac{\gamma}{\tau}(\tau_x, \tau_y) \tag{6.82}$$

where γ and τ are related by

$$\tau = \tau_Y \left(\frac{\gamma}{\gamma_Y}\right)^N \tag{6.83}$$

in which N is the hardening exponent and γ is

$$\gamma = \sqrt{\gamma_x^2 + \gamma_y^2} \tag{6.84}$$

Now we have four equations in Eqs. (6.62), (6.80), and (6.82) for the two stresses and two strains with τ and γ given in Eqs. (6.81) and (6.84), respectively, and is related by Eq. (6.83).

In the following analytical treatment, we also express the stress and strain vectors in terms of their magnitude and angle. For the stress vector (τ_x, τ_y), we have

$$(\tau_x, \tau_y) = \tau\,(\cos(\phi + \pi/2),\ \sin(\phi + \pi/2)) = \tau(-\sin\phi, \cos\phi) \tag{6.85}$$

where τ is the magnitude of the stress vector and $\phi + \pi/2$ is the angle between the positive x-axis and the vector. It follows from this expression and Eq. (6.82) that

$$(\gamma_x, \gamma_y) = \gamma(-\sin\phi, \cos\phi) \tag{6.86}$$

Here γ is the magnitude of the strain vector (γ_x, γ_y) and $\phi + \pi/2$ is also the angle between the x-axis and the strain vector.

Analytical solutions of the nonlinear plasticity equations described in the preceding are usually not available. For the Mode III SSY crack problem, however, we are able to convert the basic nonlinear equations to linear ones that may admit closed-form solutions. To this end, we do not directly solve for the stresses and strains as functions of coordinates x and y. Instead, we try to solve for x and y as functions of the strains, that is,

$$\begin{aligned} x &= x(\gamma_x, \gamma_y) \\ y &= y(\gamma_x, \gamma_y) \end{aligned} \tag{6.87}$$

which, in general, give the strains in implicit forms. Now we need to write all the basic equations in the strain plane instead of the physical plane. Taking the derivatives of both sides in Eq. (6.87) with respective to x, we have

$$\begin{aligned} 1 &= \frac{\partial x}{\partial \gamma_x}\frac{\partial \gamma_x}{\partial x} + \frac{\partial x}{\partial \gamma_y}\frac{\partial \gamma_y}{\partial x} \\ 0 &= \frac{\partial y}{\partial \gamma_x}\frac{\partial \gamma_x}{\partial x} + \frac{\partial y}{\partial \gamma_y}\frac{\partial \gamma_y}{\partial x} \end{aligned}$$

Solving these equations for $\partial \gamma_y / \partial x$, we have

$$\frac{\partial \gamma_y}{\partial x} = -\frac{1}{\Delta}\frac{\partial y}{\partial \gamma_x} \tag{6.88}$$

where Δ is the determinant of the Jacobian matrix of the transformation

$$\Delta = \frac{\partial x}{\partial \gamma_x}\frac{\partial y}{\partial \gamma_y} - \frac{\partial y}{\partial \gamma_x}\frac{\partial x}{\partial \gamma_y}$$

Δ is not zero if we have one-to-one transformation between the physical plane and the strain plane. Similarly, taking the derivatives of Eq. (6.87) with respect to y leads to

$$\begin{aligned} 0 &= \frac{\partial x}{\partial \gamma_x}\frac{\partial \gamma_x}{\partial y} + \frac{\partial x}{\partial \gamma_y}\frac{\partial \gamma_y}{\partial y} \\ 1 &= \frac{\partial y}{\partial \gamma_x}\frac{\partial \gamma_x}{\partial y} + \frac{\partial y}{\partial \gamma_y}\frac{\partial \gamma_y}{\partial y} \end{aligned}$$

Solving the equations for $\partial \gamma_x / \partial y$ yields

$$\frac{\partial \gamma_x}{\partial y} = -\frac{1}{\Delta}\frac{\partial x}{\partial \gamma_y} \tag{6.89}$$

Substituting Eqs. (6.88) and (6.89) into Eq. (6.80), we obtain the compatibility equation in the strain plane

$$\frac{\partial x}{\partial \gamma_y} - \frac{\partial y}{\partial \gamma_x} = 0 \tag{6.90}$$

Similarly, the equilibrium equation, that is, (6.62), may be written in the stress plane using the same procedure described here

$$\frac{\partial x}{\partial \tau_x} + \frac{\partial y}{\partial \tau_y} = 0 \tag{6.91}$$

The compatibility equation (6.90) is automatically satisfied with the following defined strain function $\psi = \psi(\gamma_x, \gamma_y)$

$$x = \frac{\partial \psi}{\partial \gamma_x}, \quad y = \frac{\partial \psi}{\partial \gamma_y} \tag{6.92}$$

These relations may also be written in terms of γ and ϕ using Eq. (6.86)

$$\begin{aligned} x &= -\sin\phi \frac{\partial \psi}{\partial \gamma} - \frac{\cos\phi}{\gamma} \frac{\partial \psi}{\partial \phi} \\ y &= \cos\phi \frac{\partial \psi}{\partial \gamma} - \frac{\sin\phi}{\gamma} \frac{\partial \psi}{\partial \phi} \end{aligned} \tag{6.93}$$

or

$$\bar{z} = x - iy = re^{-i\theta} = -e^{-i\phi}\left(\frac{1}{\gamma}\frac{\partial \psi}{\partial \phi} + i\frac{\partial \psi}{\partial \gamma}\right) \tag{6.94}$$

Substituting Eq. (6.93) into the equilibrium equation (6.91) and considering the following relation

$$\begin{aligned} \frac{\partial ()}{\partial \tau_x} &= -\sin\phi \frac{\partial ()}{\partial \tau} - \frac{\cos\phi}{\tau} \frac{\partial ()}{\partial \phi} \\ \frac{\partial ()}{\partial \tau_y} &= \cos\phi \frac{\partial ()}{\partial \tau} - \frac{\sin\phi}{\tau} \frac{\partial ()}{\partial \phi} \end{aligned} \tag{6.95}$$

we have

$$\frac{\tau}{\gamma \tau'(\gamma)} \frac{\partial^2 \psi}{\partial \gamma^2} + \frac{1}{\gamma}\frac{\partial \psi}{\partial \gamma} + \frac{1}{\gamma^2}\frac{\partial^2 \psi}{\partial \phi^2} = 0 \tag{6.96}$$

In the plastic zone ($\tau \geq \tau_Y$, or $\gamma \geq \gamma_Y$),

$$\tau'(\gamma) = N\frac{\tau_Y}{\gamma_Y}\left(\frac{\gamma}{\gamma_Y}\right)^{N-1}$$

Substituting the preceding equation into Eq. (6.96), we obtain the governing equation for the strain function ψ

$$\frac{1}{N}\frac{\partial^2 \psi}{\partial \gamma^2} + \frac{1}{\gamma}\frac{\partial \psi}{\partial \gamma} + \frac{1}{\gamma^2}\frac{\partial^2 \psi}{\partial \phi^2} = 0, \quad \gamma \geq \gamma_Y \tag{6.97}$$

This is a linear partial differential equation for the strain function ψ. In the elastic zone ($\tau < \tau_Y$, or $\gamma < \gamma_Y$),

$$\frac{\partial^2\psi}{\partial\gamma^2} + \frac{1}{\gamma}\frac{\partial\psi}{\partial\gamma} + \frac{1}{\gamma^2}\frac{\partial^2\psi}{\partial\phi^2} = 0, \quad \gamma < \gamma_Y \tag{6.98}$$

which is actually a Laplace equation in the strain plane. After solving the previous equations for ψ under appropriate boundary conditions, the relations between γ, ϕ and x, y may be established.

6.8.2 Boundary Conditions of SSY

The SSY condition is still given in Eq. (6.71), or equivalently

$$\gamma_y + i\gamma_x = \frac{1}{\mu}(\tau_y + i\tau_x) \to \frac{K_{III}}{\mu\sqrt{2\pi z}}, \quad |z|/R_p \to \infty \tag{6.99}$$

where R_p is a measure of the plastic zone size. The asymptotic condition at $|z|/R_p \to \infty$ means that we can consider a semi-infinite plane (after symmetry consideration) for the SSY crack problem, as shown earlier in Figure 6.14.

The crack face traction-free condition now becomes

$$\tau_y = 0, \qquad y = 0,\ x < 0 \tag{6.100}$$

and the symmetry condition along the crack line is

$$w = 0, \qquad y = 0,\ x > 0 \tag{6.101}$$

Using Hooke's law (6.64), the elastic-plastic stress–strain relationship (6.82), and the strain-displacement relation (6.63), the conditions in Eqs. (6.100) and (6.101) can be expressed in the following equivalent forms

$$\gamma_y = 0, \qquad y = 0,\ x < 0 \tag{6.102}$$

$$\gamma_x = 0, \qquad y = 0,\ x > 0 \tag{6.103}$$

Because we are dealing with a crack problem, a strain singularity at the tip ($z = 0$) is anticipated, that is,

$$\gamma \to \infty, \quad z \to 0 \tag{6.104}$$

Finally, we require that the stresses and strains be continuous across the elastic-plastic boundary, in other words,

$$[[\gamma_x]] = 0, \quad [[\gamma_y]] = 0 \tag{6.105}$$

where $[[\gamma_x]]$ and $[[\gamma_y]]$ represent the discontinuities of γ_x and γ_y across the elastic-plastic boundary, respectively.

Using Eq. (6.86), the boundary conditions in Eqs. (6.103) and (6.102) can be rewritten in terms of ϕ as follows

$$\phi = 0, \qquad y = 0,\ x > 0 \tag{6.106}$$

$$\phi = \frac{\pi}{2}, \qquad y = 0,\ x < 0 \tag{6.107}$$

respectively. Hence, the physical half plane, $y > 0$, is mapped onto the quarter plane

$$0 < \phi < \pi/2$$

in the strain plane, as shown in Figure 6.15. By noting Eq. (6.93), the symmetry condition in Eq. (6.106) in the strain plane becomes

$$\frac{\partial \psi}{\partial \gamma} = 0, \qquad \phi = 0 \tag{6.108}$$

and the traction-free condition (6.107) becomes

$$\frac{\partial \psi}{\partial \phi} = 0, \qquad \phi = \frac{\pi}{2} \tag{6.109}$$

The SSY condition in the strain plane follows from Eq. (6.99)

$$z \to \frac{K_{III}^2}{2\pi\mu^2} \frac{1}{(\gamma_y + i\gamma_x)^2}, \quad \gamma \to 0$$

or by noting Eq. (6.94) and $\gamma_y + i\gamma_x = \gamma e^{-i\phi}$

$$-e^{-i\phi}\left(\frac{1}{\gamma}\frac{\partial \psi}{\partial \phi} + i\frac{\partial \psi}{\partial \gamma}\right) \to \frac{K_{III}^2}{2\pi\mu^2\gamma^2} e^{-2i\phi}, \quad \gamma \to 0$$

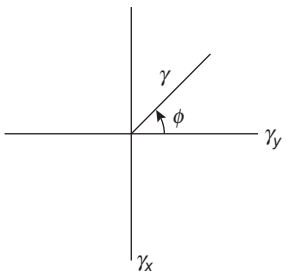

FIGURE 6.15

Strain vector in the strain plane.

The preceding condition can be further simplified as follows

$$\psi \to -\frac{K_{III}^2}{2\pi\mu^2}\frac{\sin\phi}{\gamma}, \quad \gamma \to 0 \tag{6.110}$$

The asymptotic condition at the crack tip (6.104) and the transformation (6.94) imply that the strain function ψ has the asymptotic properties

$$\frac{\partial\psi}{\partial\gamma} \to 0, \quad \frac{1}{\gamma}\frac{\partial\psi}{\partial\phi} \to 0, \qquad \gamma \to \infty \tag{6.111}$$

The stress or strain continuity conditions (6.105), together with Eqs. (6.86) and (6.94), mean that both ψ and $\partial\psi/\partial\gamma$ remain continuous across the elastic-plastic boundary (described by $\gamma = \gamma_Y$ in the strain plane)

$$[[\psi]] = 0, \quad \left[\left[\frac{\partial\psi}{\partial\gamma}\right]\right] = 0, \qquad \gamma = \gamma_Y \tag{6.112}$$

6.8.3 Elastic-Plastic Solution

The elastic-plastic Mode III crack problem now reduces to finding the solution of governing equations, (6.98) and (6.97), in the elastic and plastic zones, respectively, under the conditions in Eqs. (6.108) through (6.112).

In the elastic region, the SSY condition (6.110) and the boundary conditions (6.108) and (6.109) suggest that the strain function ψ may be expressed in the following separable form

$$\psi(\gamma,\phi) = f(\gamma)\sin\phi \tag{6.113}$$

where $f(\gamma)$ is a function of the magnitude of the strain vector. Substituting this equation into Eq. (6.98) yields the following equation for $f(\gamma)$

$$\frac{d^2f}{d\gamma^2} + \frac{1}{\gamma}\frac{df}{d\gamma} - \frac{f}{\gamma^2} = 0, \quad \gamma < \gamma_Y$$

The general solution of the equation is

$$f(\gamma) = C_1\gamma^{-1} + C_2\gamma$$

where C_1 and C_2 are unknown constants to be determined. The general solution of ψ in the elastic zone thus can be expressed as

$$\psi(\gamma,\phi) = \left(C_1\gamma^{-1} + C_2\gamma\right)\sin\phi, \quad \gamma < \gamma_Y \tag{6.114}$$

In the plastic zone, the strain function ψ may still be expressed in the separable form (6.113) from the consideration of continuity conditions across the elastic-plastic

boundary. Substituting ψ from Eq. (6.113) into the basic equation (6.97) yields the following equation for $f(\gamma)$ in the plastic zone

$$\frac{1}{N}\frac{d^2f}{d\gamma^2}+\frac{1}{\gamma}\frac{df}{d\gamma}-\frac{f}{\gamma^2}=0, \quad \gamma \geq \gamma_Y$$

with the following general solution

$$f(\gamma)=C_3\gamma^{-N}+C_4\gamma$$

where C_3 and C_4 are constants to be determined. The general solution of ψ in the plastic zone can be expressed as

$$\psi(\gamma,\phi)=\left(C_3\gamma^{-N}+C_4\gamma\right)\sin\phi, \quad \gamma \geq \gamma_Y \tag{6.115}$$

Clearly, the general solutions in Eqs. (6.114) and (6.115) satisfy the boundary conditions in Eqs. (6.108) and (6.109). We now determine the unknown constants $C_i(i=1,2,3,4)$ using conditions Eqs. (6.110) through (6.112). It follows from the SSY condition (6.110) and the solution in the elastic zone (6.114) that

$$C_1=-\frac{K_{III}^2}{2\pi\mu^2}=-\frac{K_{III}^2\gamma_Y^2}{2\pi\tau_Y^2}$$

The asymptotic condition in Eq. (6.111) and the solution in the plastic zone (6.115) give

$$C_4=0$$

According to the continuity requirements (6.112), the remaining two constants C_2 and C_3 satisfy the following conditions after using the ones in obtained C_1 and C_4

$$-\frac{K_{III}^2\gamma_Y^2}{2\pi\tau_Y^2}\gamma_Y^{-1}+C_2\gamma_Y=C_3\gamma_Y^{-N}, \qquad \frac{K_{III}^2\gamma_Y^2}{2\pi\tau_Y^2}\gamma_Y^{-2}+C_2=-NC_3\gamma_Y^{-N-1}$$

Solving these equations for C_2 and C_3, we obtain

$$C_2=-\frac{K_{III}^2}{2\pi\tau_Y^2}\frac{1-N}{1+N}, \qquad C_3=-\frac{K_{III}^2}{\pi\tau_Y^2}\frac{\gamma_Y^{N+1}}{(1+N)}$$

Using these determined constants, we have the solution for the strain function ψ as follows

$$\psi(\gamma,\phi)=-\frac{K_{III}^2}{\pi\tau_Y^2}\frac{\gamma_Y}{(1+N)}\left(\frac{\gamma_Y}{\gamma}\right)^N\sin\phi, \quad \gamma \geq \gamma_Y \tag{6.116}$$

$$\psi(\gamma,\phi)=-\frac{K_{III}^2\gamma_Y}{2\pi\tau_Y^2}\left(\frac{\gamma_Y}{\gamma}+\frac{1-N}{1+N}\frac{\gamma}{\gamma_Y}\right)\sin\phi, \quad \gamma < \gamma_Y \tag{6.117}$$

With the previously solved strain function ψ, we can obtain the stresses and strains for the Mode III SSY elastic-plastic crack problem. Substituting the solution in the plastic zone (6.116) into Eq. (6.94) yields

$$\begin{aligned} re^{-i\theta} &= e^{-i\phi}\frac{K_{III}^2}{\pi\tau_Y^2}\frac{1}{(1+N)}\left(\frac{\gamma_Y}{\gamma}\right)^{N+1}(\cos\phi - iN\sin\phi) \\ &= \frac{K_{III}^2}{\pi\tau_Y^2}\frac{1}{(1+N)}\left(\frac{\gamma_Y}{\gamma}\right)^{N+1}\left(\frac{1-N}{2}+\frac{1+N}{2}e^{-2i\phi}\right) \end{aligned}$$

or

$$\begin{aligned} x = r\cos\theta &= \frac{K_{III}^2}{2\pi\tau_Y^2}\left(\frac{\gamma_Y}{\gamma}\right)^{N+1}\left[\frac{1-N}{1+N}+\cos 2\phi\right] \\ y = r\sin\theta &= \frac{K_{III}^2}{2\pi\tau_Y^2}\left(\frac{\gamma_Y}{\gamma}\right)^{N+1}\sin 2\phi \end{aligned} \tag{6.118}$$

The implicit solutions of γ and ϕ in the plastic zone can be obtained from Eq. (6.118) as follows

$$\sin(2\phi-\theta) = \frac{1-N}{1+N}\sin\theta \tag{6.119}$$

$$\frac{\gamma}{\gamma_Y} = \left(\frac{K_{III}^2}{2\pi\tau_Y^2}\frac{1}{r}\right)^{\frac{1}{1+N}}\left(\frac{\sin 2\phi}{\sin\theta}\right)^{\frac{1}{1+N}} \tag{6.120}$$

Substituting Eq. (6.120) into Eq. (6.86) yields the strains in the plastic zone

$$\begin{aligned} \gamma_x &= -\gamma_Y\left(\frac{K_{III}^2}{2\pi\tau_Y^2}\frac{1}{r}\right)^{\frac{1}{1+N}}\left(\frac{\sin 2\phi}{\sin\theta}\right)^{\frac{1}{1+N}}\sin\phi \\ \gamma_y &= \gamma_Y\left(\frac{K_{III}^2}{2\pi\tau_Y^2}\frac{1}{r}\right)^{\frac{1}{1+N}}\left(\frac{\sin 2\phi}{\sin\theta}\right)^{\frac{1}{1+N}}\cos\phi \end{aligned} \tag{6.121}$$

The stresses can be obtained by subsituting Eq. (6.120) into the power law (6.83) and then Eq. (6.85) as follows

$$\begin{aligned} \tau_x &= -\tau_Y\left(\frac{K_{III}^2}{2\pi\tau_Y^2}\frac{1}{r}\right)^{\frac{N}{1+N}}\left(\frac{\sin 2\phi}{\sin\theta}\right)^{\frac{N}{1+N}}\sin\phi \\ \tau_y &= \tau_Y\left(\frac{K_{III}^2}{2\pi\tau_Y^2}\frac{1}{r}\right)^{\frac{N}{1+N}}\left(\frac{\sin 2\phi}{\sin\theta}\right)^{\frac{N}{1+N}}\cos\phi \end{aligned} \tag{6.122}$$

In the elastic zone, γ and ϕ may be obtained by substituting Eq. (6.117) into Eq. (6.94) as follows

$$\bar{z} = re^{-i\theta} = \frac{K_{III}^2}{2\pi\tau_Y^2}\left[\left(\frac{\gamma_Y}{\gamma}\right)^2 e^{-2i\phi} + \frac{1-N}{1+N}\right] \tag{6.123}$$

This equation becomes the following after using Eq. (6.86)

$$z - \frac{1-N}{1+N}\frac{K_{III}^2}{2\pi\tau_Y^2} = \frac{K_{III}^2}{2\pi\tau_Y^2}\left(\frac{\gamma_Y}{\gamma}\right)^2 e^{2i\phi} = \frac{K_{III}^2}{2\pi\tau_Y^2}\left(\frac{\gamma_Y}{\gamma_y + i\gamma_x}\right)^2 \tag{6.124}$$

The strains and hence stresses in the elastic zone can thus be obtained as follows

$$\gamma_y + i\gamma_x = \frac{K_{III}}{\mu}\frac{1}{\sqrt{2\pi\left(z - \frac{1-N}{1+N}\frac{K_{III}^2}{2\pi\tau_Y^2}\right)}} \tag{6.125}$$

$$\tau_y + i\tau_x = \frac{K_{III}}{\sqrt{2\pi\left(z - \frac{1-N}{1+N}\frac{K_{III}^2}{2\pi\tau_Y^2}\right)}} \tag{6.126}$$

Finally, the elastic-plastic boundary may be determined by equating γ in Eq. (6.124) to γ_Y as follows

$$z - X_0 = R_0 e^{2i\phi} \tag{6.127}$$

where X_0 and R_0 are given by

$$X_0 = \frac{1-N}{1+N}\frac{K_{III}^2}{2\pi\tau_Y^2}, \qquad R_0 = \frac{K_{III}^2}{2\pi\tau_Y^2} \tag{6.128}$$

Equation (6.127) represents a circle of radius R_0 centered at $x = X_0$ on the x-axis as shown in Figure 6.16. The plastic zone size ahead of the crack is

$$R_p = X_0 + R_0 = \frac{1}{(1+N)\pi}\left(\frac{K_{III}}{\tau_Y}\right)^2$$

In summary, the Mode III small-scale yielding solutions for the elastic power-law material indicate that

1. The plastic zone has a circular shape with a radius of $(K_{III}/\tau_Y)^2/(2\pi)$ centered on the x-axis at $(1-N)(K_{III}/\tau_Y)^2/(2\pi(1+N))$. The crack tip is in the plastic zone.
2. The stresses and strains are singular at the crack tip, $r = 0$, according to $r^{-N/(1+N)}$ and $r^{-1/(1+N)}$, respectively.
3. The solution reduces to that for the elastic perfectly plastic material in Section 6.7 when the hardening exponent $N \to 0$.

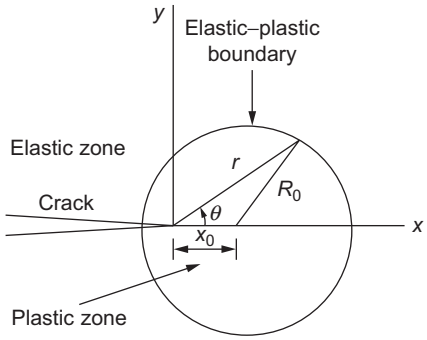

FIGURE 6.16

Plastic zone near the tip of a Mode III crack in an elastic power-law hardening material under small scale yielding.

6.9 HRR FIELD

In elastic-plastic fracture mechanics, a parallel issue to the elastic crack tip K-field is the stress and deformation fields near a crack tip in an elastic-plastic material. Rice and Rosengren [6-6] and Hutchinson [6-7] studied the Mode I problem for a power-law hardening material in the framework of deformation plasticity and obtained the near-tip stress and deformation fields, which are commonly called the HRR field.

Consider a crack in an elastic power-law hardening material as shown in Figure 6.17. The material is assumed to follow the Ramberg-Osgood model in uniaxial loading,

$$\frac{e}{e_Y} = \frac{\sigma}{\sigma_Y} + \alpha \left(\frac{\sigma}{\sigma_Y} \right)^n \tag{6.129}$$

where α is a dimensionless material parameter and n is the hardening exponent. The stress–strain relationship of the deformation plasticity Eqs. (6.26) and (6.27) may be rewritten as

$$e_{ij} = \frac{1+\nu}{E}\sigma_{ij} - \frac{\nu}{E}\sigma_{kk}\delta_{ij} + \frac{3}{2}\frac{\overline{e^p}}{\overline{\sigma}}\sigma'_{ij} \tag{6.130}$$

For the material following the Ramberg-Osgood model Eq. (6.129), Eq. (6.130) reduces to

$$e_{ij} = \frac{1+\nu}{E}\sigma_{ij} - \frac{\nu}{E}\sigma_{kk}\delta_{ij} + \frac{3}{2}\alpha e_Y \left(\frac{\overline{\sigma}}{\sigma_Y} \right)^{n-1} \frac{\sigma'_{ij}}{\sigma_Y} \tag{6.131}$$

Assume stresses have the following asymptotic form near the crack tip:

$$\sigma_{ij} = \sigma_Y A r^{\lambda} \tilde{\sigma}_{ij}(\theta), \quad r \to 0 \tag{6.132}$$

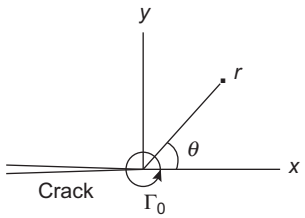

FIGURE 6.17

Coordinate systems at a crack tip.

where A is a constant, $\lambda < 0$ is a singularity exponent, $\tilde{\sigma}_{ij}(\theta)$ are the angular distributions, and (r,θ) are the polar coordinates centered at the crack tip, see Figure 6.17. Substituting the previous asymptotic expression into the constitutive law Eq. (6.131), we see that the plastic strain has a stronger singularity than the elastic strain, which thus can be neglected in the near-tip singular fields. Equation (6.131) is then reduced to the following simpler form in the near-tip region:

$$e_{ij} = \frac{3}{2}\alpha e_Y \left(\frac{\overline{\sigma}}{\sigma_Y}\right)^{n-1} \frac{\sigma'_{ij}}{\sigma_Y} \tag{6.133}$$

and the strains have the asymptotic form near the crack tip:

$$e_{ij} = \alpha e_Y A^n r^{\lambda n} \tilde{e}_{ij}(\theta), \qquad r \to 0 \tag{6.134}$$

To determine the singularity exponent λ, first evaluate the strain energy density W near the crack tip. It follows from Eqs. (6.132) through (6.134) that

$$W = \int_0^{e_{ij}} \sigma_{ij} de_{ij} = \alpha \sigma_Y e_Y \frac{n}{n+1} \left(\frac{\overline{\sigma}}{\sigma_Y}\right)^{n+1} \to r^{\lambda(n+1)} \tilde{W}(\theta), \quad r \to 0 \tag{6.135}$$

Recall that the J-integral is the energy release rate for nonlinear elastic materials and the stress–strain relation Eq. (6.133) is essentially a kind of nonlinear elastic constitutive law. Evaluating J along a circle surrounding the crack tip, we have

$$J = r \int_{-\pi}^{\pi} \left[W \cos\theta - \sigma_{ij} n_j \frac{\partial u_i}{\partial x} \right] d\theta \tag{6.136}$$

For J to be nonzero and finite, the integrand in this integral should have a singularity of $1/r$ at the crack tip, that is,

$$W \to \frac{\tilde{W}(\theta)}{r}, \quad r \to 0 \tag{6.137}$$

The singularity exponent λ is thus determined by observing Eqs. (6.135) and (6.137):

$$\lambda = -\frac{1}{n+1}$$

Substituting this exponent into Eqs. (6.132) and (6.134) yields the following near-tip stress and strain fields:

$$\sigma_{ij} = \sigma_Y A r^{-\frac{1}{n+1}} \tilde{\sigma}_{ij}(\theta), \qquad r \to 0 \tag{6.138}$$

$$e_{ij} = \alpha e_Y A^n r^{-\frac{n}{n+1}} \tilde{e}_{ij}(\theta), \qquad r \to 0 \tag{6.139}$$

The stress and strain angular distribution functions $\tilde{\sigma}_{ij}$ and $\tilde{e}_{ij}$ in Eqs. (6.138) and (6.139) may be obtained by using the equilibrium equations, the strain compatibility condition, the stress–strain relation in Eq. (6.133), and the appropriate boundary conditions; see Rice and Rosengren [6-6] and Hutchinson [6-7]. These angular distributions also depend on the hardening exponent n. The amplitude constant A can be determined by substituting the asymptotic stresses and strains in Eqs. (6.138) and (6.139) into Eq. (6.136) with the result

$$J = \alpha \sigma_Y e_Y A^{n+1} I_n$$

where I_n is a known constant depending on the hardening exponent n. The final forms of the HRR field can be expressed as follows:

$$\sigma_{ij} = \sigma_Y \left(\frac{J}{\alpha \sigma_Y e_Y I_n r} \right)^{\frac{1}{n+1}} \tilde{\sigma}_{ij}(\theta, n), \quad r \to 0 \tag{6.140}$$

$$e_{ij} = \alpha e_Y \left(\frac{J}{\alpha \sigma_Y e_Y I_n r} \right)^{\frac{n}{n+1}} \tilde{e}_{ij}(\theta, n), \quad r \to 0 \tag{6.141}$$

$$u_i = \alpha e_Y \left(\frac{J}{\alpha \sigma_Y e_Y I_n} \right)^{\frac{n}{n+1}} r^{\frac{1}{n+1}} \tilde{u}_i(\theta, n), \quad r \to 0 \tag{6.142}$$

The HRR field shows that (1) the stresses have a singularity of $r^{-1/(n+1)}$ at the crack tip in a power-law hardening material, and (2) the intensity of the singular stress field is characterized by the J-integral.

6.10 ENERGY RELEASE RATE CONCEPT IN ELASTIC-PLASTIC MATERIALS

Energy release rate plays a very important role in Griffith's theory of fracture. It is a common notion that a crack extends because of the surplus energy released to provide the energy needed in creating new surfaces during crack growth. From the energy balance point of view, we have accepted that, during crack extension of Δa,

the work done by external forces ΔW_e is equal to the sum of the increase of elastic strain energy ΔU and the energy released ΔW_s. However, within the framework of classical elasticity, there is no mechanism that is capable of storing surface energy. Therefore, released energy should be absent from the body after crack extension, and, as a result, the energy balance requirement during crack extension cannot be satisfied.

Extending the Griffith energy balance concept for fracture in elastic-plastic solids, we have

$$\Delta W_e = \Delta U + \Delta W_s + \Delta W_p \tag{6.143}$$

in which ΔW_p is the increment of plastic dissipation work. Using the finite element analysis, Sun and Wang [6-8] showed that the energy balance (Eq. 6.143) is satisfied with $\Delta W_s = 0$. They consider a rectangular panel containing a center crack subjected to uniform tension. The applied stress is kept constant during crack extension. A state of plane stress is assumed, and the four-node plane stress element is used to model the panel. For low loading levels, finer meshes are used to capture the small plastic zone.

The material is elastic-perfectly plastic following the von Mises yield criterion and the associated flow rule. Unloading is elastic following the initial modulus of elasticity. The material constants are given by Young's modulus $E = 207$ GPa, Poisson's ratio $\nu = 0.32$, and the yield stress $\sigma_Y = 310$ MPa.

As shown in Figure 6.18, the crack tip is to grow from position A to position B by an amount Δa. To simulate the continuous crack growth process, essentially a large number of extension steps must be performed from A to B. In other words, each numerical nodal release step δa must be sufficiently small to capture the work done during the continuous advance of the plastic zone ahead of the crack tip. The plastic dissipation work is underestimated if the extension step is not sufficiently small.

Figure 6.19 shows the relationships between ratios of energy rates versus $\delta a/R_p$. The energy rates are defined in a manner similar to the enegy release rate, by

$$G_s = \Delta W_s / \Delta a$$

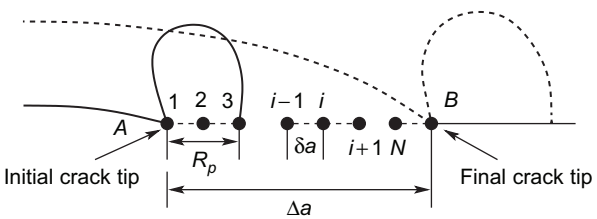

FIGURE 6.18

Crack extension in an elastic-plastic material (Δa is the total growth length and δa is the growth length per extension step).

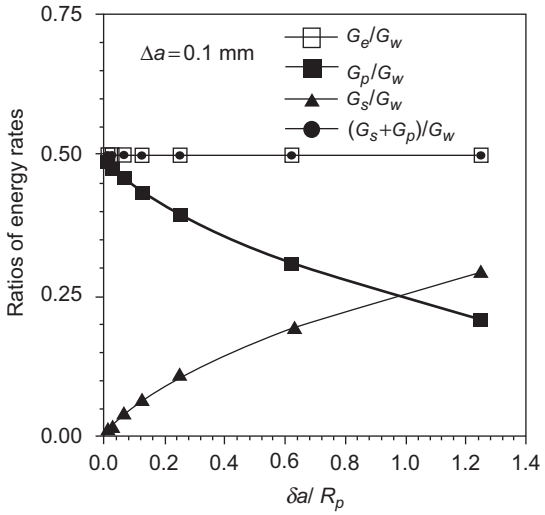

FIGURE 6.19

Ratios of energy rates versus $\delta a/R_p$ (adapted from Sun and Wang [6-8]).

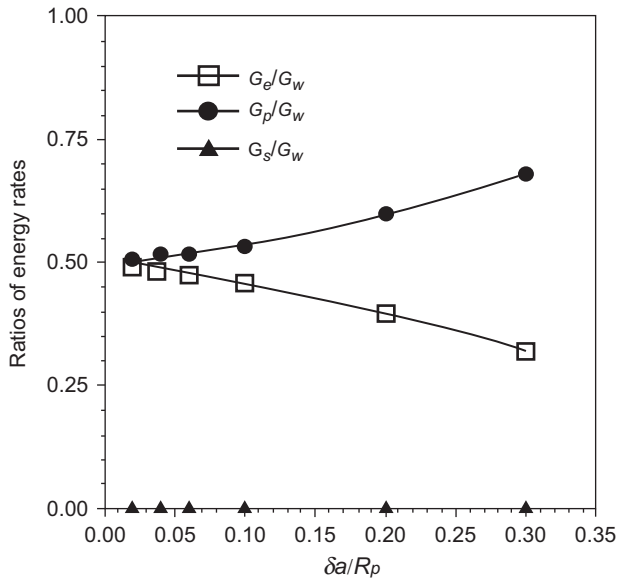

FIGURE 6.20

Effects of plastic zone size on the ratios of energy rates (adapted from Sun and Wang [6-8]).

and

$$G_w = \Delta W_e / \Delta a$$
$$G_p = \Delta W_p / \Delta a$$
$$G_e = \Delta U / \Delta a$$

It is found that G_s approaches zero and G_p approaches the value of G_e as $\delta a / R_p$ decreases. Of course, theoretically the converged solution is obtained with $\delta a \to 0$. These results indicate that, according to the continuum elastoplasticity model, there is no surplus energy released during crack extension and that the only mechanism for energy dissipation during crack extension is plastic work.

It is of interest to investigate the result taking the elastic solution as a limiting case of the elastic-plastic solution. This may be achieved by greatly raising the value of the yield stress, or making the crack tip plastic zone size very small. The finite element method results are shown in Figure 6.20. First, we note that the separation work (energy release) vanishes independent of the plastic zone size. As the plastic zone size increases, the plastic dissipation work rate increases while the elastic strain energy variation rate decreases.

It is interesting to note that, as R_p approaches zero, both G_e and G_p approach 1/2. This means that the elastic energy release rate G_s, which is equal to G in LEFM, is equal to the plastic dissipation work rate when an elastic solid is considered as a limiting case of an elastic-perfectly plastic solid by taking $R_p \to 0$. Thus, the difference between G_p and G may be used as a quantitative measure of the validity of the small-scale yielding concept.

References

[6-1] G.R. Irwin, Plastic zone near a crack and fracture toughness, in: Proceedings of the 7th Sagamore Ordnance Materials Conference, Syracuse University, Syracuse, New York, 1960, pp. IV-63–IV-78.

[6-2] D.S. Dugdale, Yielding of steel sheets containing slits, J. Mech. Phys. Sol. 8 (1960) 100–104.

[6-3] F.M. Burdekin, D.E.W. Stone, The crack opening displacement approach to fracture mechanics in yielding materials, J. Strain Anal. 1 (1966) 145–153.

[6-4] H-O. Kim, Elastic-plastic fracture analysis for small scale yielding, PhD thesis, School of Aeronautics and Astronautics, Purdue University, West Lafayette, IN, 1996.

[6-5] J.A.H. Hult, F.A. McClintock, Elastic-plastic stress and strain distributions around sharp notches under repeated shear, in: Proceedings of the 9th International Congress for Applied Mechanics, Vol. 8, 1957, pp. 51–58.

[6-6] J.R. Rice, G.F. Rosengren, Plane strain deformation near a crack tip in a power-law hardening material, J. Mech. Phys. Sol. 16 (1968) 1–12.

[6-7] J.W. Hutchinson, Singular behavior at the end of a tensile crack in a hardening material, J. Mech. Phys. Sol. 16 (1968) 13–31.

[6-8] C.T. Sun and C.Y. Wang, A new look at energy release rate in fracture mechanics, Inter. J. Fract. 113 (2002) 295–307.

[6-9] J.R. Rice, Stresses due to a sharp notch in a work-hardening elastic-plastic material loaded by longitudinal shear, J. Appl. Mech. 34 (1967) 287–298.

PROBLEMS

6.1 A split beam of 2 mm wide is loaded as shown in Figure 6.21. Assume that the yield stress of the material is 500 MPa. Find the load P that produces a plastic zone size of 2 mm ahead of the crack tip, using the methods that are available to you, given Young's modulus $E = 70$ GPa.

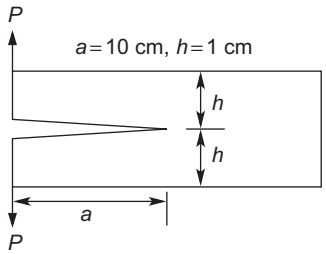

FIGURE 6.21

A split beam of elastic-plastic material.

6.2 Consider an infinite plate with a center crack subjected to a pair of concentrated forces as shown in Figure 3.8 in Chapter 3. Estimate the plastic zone sizes using Irwin's plastic zone adjustment method and the Dugdale model based on

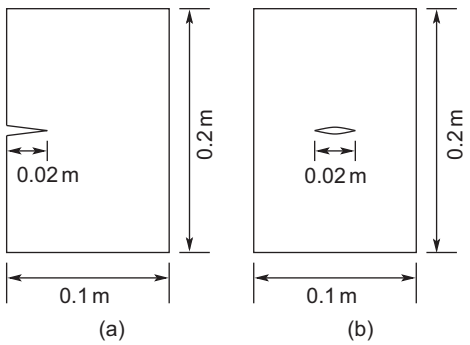

FIGURE 6.22

(a) An edge-cracked plate, and (b) a center-cracked plate.

the small-scale yielding assumption. Also derive the plastic zone size using the Dugdale model without imposing the small-scale yielding condition.

6.3 Consider an edge-cracked plate and a center-cracked panel as shown in Figure 6.22(a) and (b), respectively. Assume that both plates are subjected to a uniform tensile stress applied in the vertical direction. Use finite element analysis to determine the plastic zone size for various levels of the applied load. Assume elastic-perfectly plastic stress–strain behavior. (a) Plot the plastic zone according to plane stress and plane strain assumptions and compare with the results obtained using the elastic solutions. (b) Compare the plastic zone size (along the crack plane) at different load levels with those estimated according to Irwin's approach.